Article:
Chatterjee, J., Dionora, M.J., Laza, M.R. et al. (2026) Rice leaf structural adjustment to sustain photosynthetic traits under drought and produce more grain: Evidence from field studies of the 3K indica panel. Current Plant Biology, 50. 100660. ISSN: 2214-6628

https://doi.org/10.1016/j.cpb.2026.100660

Current Plant Biology 50 (2026) 100660

Contents lists available at ScienceDirect

Current Plant Biology

journal homepage: www.elsevier.com/locate/cpb

Rice leaf structural adjustment to sustain photosynthetic traits under drought and produce more grain: Evidence from field studies of the 3K indica panel

Jolly Chatterjee [a,1], Mary Jacqueline Dionora [a,b], Ma Rebecca Laza [a], Marjorie de Ocampo [a,2], Pauline M. Muyco [a], Maria Elizabeth B. Naredo [a,3], Mignon Natividad [a,4], Marinell Ramirez-Quintana [a,5], Dmytro Chebotarov [a,6], Stephen Klassen [a], William Paul Quick [a,c], Amelia Henry [a,d,*,7], Kenneth L. McNally [a,e,f,*,8]

[a] Rice Breeding Innovations Department, International Rice Research Institute, Los Baños, Laguna 4031, Philippines
[b] University of St. La Salle, Bacolod, Negros Occidental 6100, Philippines
[c] Department of Animal and Plant Sciences, University of Sheffield, Sheffield S10 2TN, United Kingdom
[d] UMR AGAP Institut, Univ Montpellier, CIRAD, INRAE, Institut Agro, Montpellier, France
[e] Philippine Genome Center for Agriculture, University of the Philippines Los Baños, College, Los Baños, Laguna 4031, Philippines
[f] Food Crops Research Institute, Yunnan Academy of Agricultural Sciences, Kunming 650200, China

ARTICLE INFO

Keywords:
Rice
drought
Leaf
Photosynthesis
3K rice genomes
Leaf water potential
GWAS
High throughput drone images

ABSTRACT

Understanding plant traits that contribute to maintenance of physiological activities under drought is crucial for sustainable rice production. Leaf morphological characters together with UAV-based HTP measurements of canopy temperature (CT) and NDVI, leaf water potential (ψ_{Leaf}), photosynthetic traits including *A*, g_s *E* and *Ci*, and drought response index (DRI) were collected from > 600 indica genotypes in two field dry seasons. This dataset from the 3 K rice sequenced genomes under well-watered (WW) and managed drought stress (MDS) revealed drought-induced leaf morpho-functional interactive changes related to grain yield under drought. Onset of drought caused ~14–20% reduction in *Ci* and 35 – 56% reduction in *A* causing serious loss in yield. Correlation analyses from two years of field dry seasons revealed that the combination of initially broader leaves capable of increasing leaf thickness in response to drought, as evidenced by changes in SLA, together with maintenance of ψ_{Leaf}, supporting a higher A_{net}, can collectively drive a higher DRI. The SLA changes ranged up to ~50% in one of the best performing genotypes with high DRI values upon severe drought stress. GWAS identified seven QTLs for DRI which include known drought-responsive aquaporin, dehydrin, and heat shock protein genes, which coincide with the GWAS interval identified for CT on chromosome 7. This study identified a tentative pathway linking genomic loci to water balance, leaf development, and photosynthesis-related traits under

Abbreviations: DAS, days after seeding; DAT, Days after transplanting; WW, well-watered; MDS, Managed drought stress; DS, dry season; GRWT, grain weight; WUE, water use efficiency; Anet, leaf level net photosynthesis; SLA, specific leaf area; LWP, Leaf water potential.

* Corresponding authors at: Rice Breeding Innovations Department, International Rice Research Institute, Los Baños, Laguna 4031, Philippines.
E-mail addresses: j.chatterjee@cgiar.org (J. Chatterjee), j.dionora2@gmail.com, j.dionora@irri.org (M.J. Dionora), mrclaza@gmail.com, m.r.laza@irri.org (M.R. Laza), m.deocampo@cgiar.org (M. de Ocampo), P.Muyco@cgiar.org (P.M. Muyco), mebnaredo@gmail.com, e.naredo@irri.org (M.E.B. Naredo), m.natividad@cgiar.org (M. Natividad), m.r.quintana@cgiar.org (M. Ramirez-Quintana), d.chebotarov@cgiar.org (D. Chebotarov), stephen.p.klassen@gmail.com (S. Klassen), paulquick2323@gmail.com, w.p.quick@irri.org (W.P. Quick), amelia.henry@cirad.fr (A. Henry), kenmcn59@gmail.com, k.McNally@cgiar.org (K.L. McNally).
[1] ORCID 0000-0003-2370-4185
[2] ORCID 0009-0006-9621-3714
[3] Current address- Philippine Coconut Authority - Albay Research Center, Banao, Guinobatan, Albay, Philippines
[4] ORCID 0000-0002-4007-8035
[5] ORCID 0000-0002-3308-1906
[6] ORCID 0000-0003-1351-9453
[7] ORCID 0000-0001-6255-5480
[8] ORCID 0000-0002-9613-5537

https://doi.org/10.1016/j.cpb.2026.100660
Received 29 July 2025; Received in revised form 21 August 2026; Accepted 28 August 2026
Available online 1 September 2026

drought. Our results provide opportunities to select the best-performing rice genotypes and enhance understanding about how to improve grain yield of rice under drought by mechanistic exploration, to aid drought breeding efforts by selecting optimal haplotype combinations or gene edits.

1. Introduction

Leaves are often known as the plant organ that exhibits 'early warning' signs of drought. Some of the most prominent drought-induced above-ground responses of plants include leaf rolling, stunted growth, and loss of green leaf pigmentation (reviewed by [1,2]). Plants typically fail to maintain normal physiological activities under drought due to hydrological imbalance, which severely reduces carbon assimilation. In the case of monocots, leaves roll under drought to reduce water loss, which disturbs both normal carbon assimilation and transpiration function as those processes are linearly related [3–6]. Moreover, stomatal closure under drought drastically reduces stomatal conductance (g_s), a factor that determines the flux of gaseous carbon to be fixed through photosynthesis [7–9]. Damage to photosynthetic machinery eventually limits plant biomass, subsequently affecting grain yield. Morphological components, including the leaf size, angle, and dry mass per unit leaf area are known to have profound effects on plant photosynthetic performance under well-watered conditions [10,11], but the dynamics of these traits under drought have been explored to a lesser extent [12–14]. A growing body of literature and our previous screening efforts of large rice diversity panels support the concept that higher photosynthetic rates can result in higher biomass and grain yield [10,15,16]. However, as opposed to the attention given to root biology in drought response [17–20], the relationships among leaf morphology, photosynthesis-related traits, and genetics that result in delivering a drought tolerant physiology for producing higher grain yield has not yet been defined comprehensively.

Leaf morphological features are commonly known to affect gas exchange parameters, and transpiration-related traits [21] such as larger or thicker leaves [22–24] are often used as selectable biomarkers to improve rice yield potential [25]. The leaf hairs [26], leaf width [27], or leaf thickness have been reported [28] to increase water use efficiency,

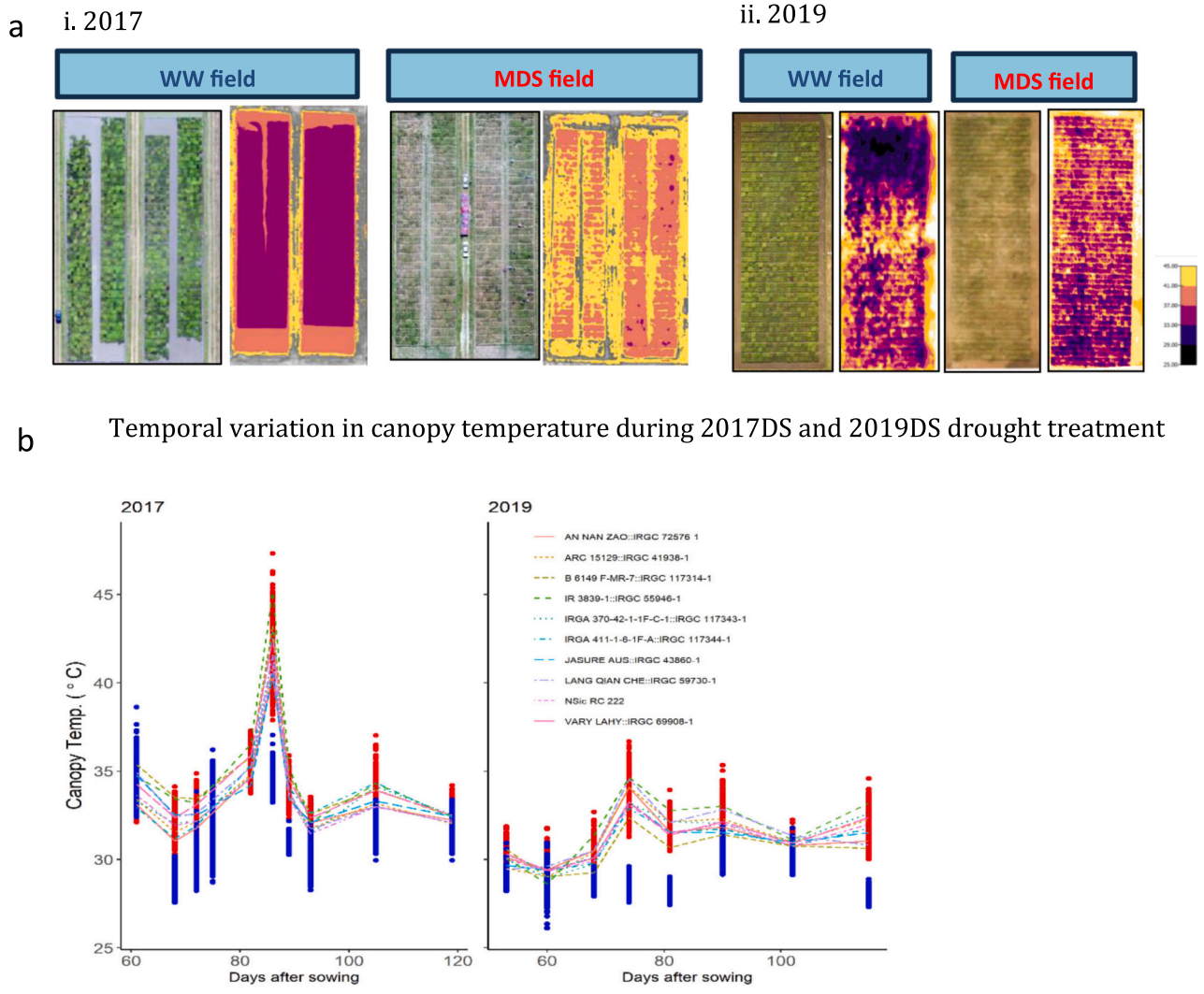

Fig. 1. (a). Representative drone RGB images and thermal images of the 3 K indica rice panel grown under well-watered (WW) and managed drought stress (MDS) fields in 2017DS (i) and 2019 DS (ii). Images were obtained at 85 DAS. (b) Canopy temperature: the lsmeans of CT, during peak drought stress, was extracted from the thermal images from drone flights. Blue and red dots are the WW_CT and MDS_CT values, respectively, at different days during the peak drought stress. Connecting lines show the canopy temperature of the best performing genotypes in our study (listed in Table S16).

which might be advantageous for plant survival under drought. Some reports identified genomic loci for rice leaf rolling (29], studied leaf reflectance and physiology [30], and leaf morphology [31], or documented response of flag leaf traits [32] under drought. However, whether altering such leaf morphological characteristics can translate into higher yield under drought remains to be tested.

Drought is considered one of the major causes of global food shortages [33] with 600 million people worldwide being predicted to face hunger in 2030; such climate change-related food security issues have thus been targeted by the United Nations Sustainable Development Goals (United Nations, 2015, https://sdgs.un.org/goals/goal5) (Accessed: 10 June 2024). Rice is one of the main crops projected to be at the highest risk of yield loss due to drought [34] especially when it occurs during reproductive stage [35]. Furthermore, the yield of the most popular drought tolerant rice varieties is still considerably low [36]. With the increasing global population, demands for food are increasing every year in both favorable and stress-prone environments. Thus, improvement of rice yield under drought stress should be a priority for breeding programs aiming to address food security under challenging climatic conditions, and an understanding of the physiological mechanisms and genetic regions related to yield under drought will aid those efforts.

Landraces often serve as potential donors in breeding to improve drought resiliency. Currently, there is a growing interest in selecting combined agro-morphological characters to complement selection for grain yield [37]. In the current study, a large-scale field trial was conducted using ~1000 rice genotypes from the sequenced 3000 Rice Genome Panel (3 K panel [38,39]:, https://snp-seek.irri.org/), including indica, aus, and admixed genotypes. This phenotypic diversity along with the availability of genomic sequences of the 3 K panel gives the opportunity to link genetics to drought responsive morphology and physiology [39]. All genotypes were evaluated in field conditions over two dry seasons for their grain yield, agronomic traits, leaf morphological traits, leaf water potential, leaf carbon assimilation, and other photosynthesis-related traits. Drone-based high-throughput RGB, multispectral, and thermal imaging traits were recorded, and a genome-wide SNP-to-trait association was performed to identify genetic loci that were best associated with maintaining crop yield under drought. In this study, we aimed 1) to understand if leaf functional traits play a role in rice drought tolerance beyond dehydration response, and 2) to identify key leaf traits and their interactions, as well as candidate genes crucial for rice drought tolerance. We hypothesized that the conservation of leaf physiological processes under drought is mediated by adaptive leaf structural changes in drought tolerant genotypes which translates to greater yield under unfavorable conditions, and this study indeed indicated that the adaptive nature of leaves was interconnected to a drought tolerant physiology. Several QTLs were identified from this study that were directly associated with higher yield under managed drought stress field conditions, which may be a valuable resource for rice drought tolerance breeding programs. Our approach using a large number of genotypes, both labor-intensive and high-throughput measurements, and the use of a field environment was intended to generate physiological and genetic insights that would be highly relevant to conditions in the target environment of drought-prone rice farmers' fields.

2. Materials and Methods

2.1. Field experiments

Indica rice genotypes were grown during the dry seasons (Jan - April) of 2017 (968 genotypes) and 2019 (578 genotypes) at the Zeigler Experimental Station of the International Rice Research Institute (IRRI; 14°10'11.81" N, 121°15'39.22" E) under both well-watered (WW) and managed drought stressed (MDS) conditions (Fig. 1a drone images). The two treatments were planted in separate fields with the genotypes arranged in partially replicated (p-rep) designs, with 20% of the genotypes replicated more than twice. Twenty-four plants of each genotype were planted per plot (0.48 m^2 area) in the field with an interplant spacing of 20 × 20 cm. The dry season drought experimental setup consisted of plot grids of 16 rows x 56 columns in 2017 and 22 rows x 48 columns in 2019, respectively, with independently randomized designs in each treatment. A detailed analysis of the well-watered component of this study is described in a companion paper by Lin et al. [40]. Varieties NSIC Rc222 (IRRI 154; high yielding), Dular (drought tolerant) and Fedearroz (Colombian popular variety) were included as checks and were randomly distributed in equal numbers across the four blocks in the field. Details of the genotypes are listed in Table S1. Plants were first raised in a seed bed nursery, followed by transplanting into the experimental field after 21 days. Basal fertilizer (complete fertilizer 14–14–14) was applied at 7 days after transplanting (DAT) followed by top dressing of urea (46−0−0) and potassium chloride (0−0−60) at 18–24 DAT. The well-watered fields were irrigated 2–3 times per week throughout the season through surface flood irrigation to maintain continuous flooding. Managed drought stress treatments were initiated by draining the water and stopping irrigation at 41 DAS in 2017DS and at 43 DAS in 2019DS. Re-watering was done after 21 days followed by a second drought stress period that continued until maturity.

Soil moisture in the MDS treatment was measured at a depth of 5–10 cm and 25–30 cm by the gravimetric method using the formula:

Soil moisture (%) = ((Weight of fresh soil – Weight of dried soil) / Weight of dried soil)*100

In 2019DS, soil moisture was additionally monitored using 6 tensiometers (SoilMoisture equipment Co. CA, USA) installed at a depth of 30 cm to record soil water potential (Ψ_{soil}). The amount of daily and total rainfall during the experiments were recorded (Table S2 and Table S3) and the soil characteristics are provided in Table S4.

2.2. Phenotyping data collection

2.2.1. High-throughput traits

Drone high-throughput phenotyping was conducted using a fixed-wing Senesefly eBee drone in 2017 and a multirotor DJI Matrice M100 drone in 2019. The eBee was flown separately using 3 different cameras as follows: RGB (senesfly SODA), 4-band multispectral (Parrot Sequoia), and Thermal (Sensefly Thermomapper). The Matrice was fitted with the following 2 cameras: RGB (DJI X3) and a 5-band multispectral (Micasense Rededge-M) capturing images simultaneously. The drones were flown weekly and images were captured at altitudes ranging from 30 to 40 m with high overlap (75–80%). Six ground control points (GCP) were placed around the perimeter of the fields for geospatial correction of the imagery. GCPs were surveyed using a high accuracy real time kinetic (RTK) GPS system (Leica Viva GS10 Base station with GS15 Smart antenna as rover). Imagery was processed using PIX4D Mapper Pro software using standard 3D mapping templates. Processing incorporated GCP correction and radiometric calibration of the multispectral imagery based on reflectance panel images taken before each flight. Processing outputs included full resolution RGB orthomosaics, digital surface models (DSM) and index maps for each camera band (WGS84 UTM 51 N coordinate system). The plot layout was digitized using ArcMap (Esri ArcGIS desktop) based on an early season RGB orthomosaic image. Plot level pixel data was extracted using R version 4.4.1 (The R Foundation for Statistical Computing, Vienna, Austria) to calculate median plot values for each camera band, vegetation indices (i.e., NDVI), field elevation, canopy height base and canopy temperature. The field elevation was based on a DSM of the field prior to transplanting. The NDVI and canopy height were calculated as follows:

$NDVI$ = (NIR – RED)/ (NIR + RED)

Canopy Height (m) = plot DSM elevation – field elevation

Table 1
The agro-morphological and physiological traits studied under well-watered and managed drought condition in two field seasons, 2017DS and 2019DS.

Category	Trait abbreviations	Definition	Units
Agronomic	DRI	Drought response index	relative unit
Agronomic	DTF	Days to 50% flowering	count
Morphological	PLHT	Height measured from base to the tip of the plants	cm
Agronomic	GRY	Grain yield, the GRWT taken at 14% moisture content per area harvested	gm / m^2
Agronomic	BM	Aboveground biomass	gm / m^2
Agronomic	HI	Harvest index (GRY / Biomass)	relative unit
Morphological	SLA	Specific leaf area	cm^2/gm
Morphological	LA	Leaf area	cm^2
Morphological	LLT	Leaf length	cm
Morphological	LWD	Leaf width	cm
Morphological	LT	Unit leaf weight which mainly corresponds to leaf thickness simulated as LA / SLA	derived character
Morphological	LDW	Leaf dry weight oven dried	gm
Physiological	LWP (Ψ_{Leaf})	Leaf water potential	Mpa
Physiological	*A* or A_{net}	Net photosynthesis	μmol CO_2 / m^2/s
Physiological	*E*	Transpiration	mmol H_2O / m^2 /s
Physiological	g_s	Stomatal conductance to H_2O	μmol H_2O / m^2/s
Physiological	*Ci*	Intercellular CO_2 concentration	ppm
Physiological	WUE or WUE_i	Instantaneous water use efficiency measured as A/ E	relative unit
Physiological	A x LT	Photosynthesis / leaf unit volume	derived character
Physiological	A/g_s	Intrinsic water use efficiency, or $_i$WUE	relative unit
Physiological	Ci/g_s	The conductance component used for controlling CO_2 in intercellular spaces	relative unit
Physiological	E/g_s	The conductance component used for transpiration	relative unit
Physiological	CT	Canopy temperature obtained from drone images	Celsius
Morphological	NDVI	Normalized difference of vegetation index obtained from drone images	relative unit

2.2.2. Agronomic and leaf morphological phenotyping

Among the agronomic traits (Table 1); Days to flowering (DTF), plant height (PLHT), grain weight (GRWT) was measured in both seasons, whereas the above-ground biomass was collected only in 2017DS. Days to flowering for each genotype was recorded when 80% of the plants in a plot were flowering. Grain weight was determined from the center plants of the 12 hills per plot to avoid any border effect. Harvested grains were dried at 40°C for three days followed by drying at 15°C for ~1 month at 15% RH. Final grain yield (GRY, g m^{-2}) at 14% seed moisture content (MC) was calculated as:

GRY at 14% MC = [grain weight (g) x (100-moisture content (%))/86]/ area harvested (m^2)

To calculate the Drought Response Index (DRI), we followed the approach of Bidinger et al [17,41] in which a predicted value of grain yield under drought was computed based on flowering time and yield under well-watered conditions, and then compared to the actual yield under drought. The grain yield under stress was converted to a predicted value (GRY_MS_predicted) based on multiple regression of each genotype's grain yield (GRY_WW) and time to flowering (DTF_WW) under well-watered conditions, in which GRY_stress_predicted = a + (b×GRYcontrol) + (c×DTFcontrol). Here, "a" is the intercept, "b" and "c" are the coefficients of the linear regression model (using the lm function in R). Next, the difference between this predicted grain yield and the actual grain yield under drought stress was used to calculate DRI:

DRI = (GRY_MS_actual – GRY_MS_predicted)/ S.E. of GRY_MS_predicted,

The R scripts and detailed description of the DRI calcuations are shown in Table S6 and Table S7.

Biomass data was collected in 2017DS after drying the above ground plant biomass (panicles+straw) at 40°C for three days. The biomass data and grain yield data were used to calculate harvest index (HI) as the ratio of grain yield to total shoot dry matter as:

HI = GRY / Biomass

Morphological and agronomic traits were measured as described previously in the phenotypic "data dictionary" for the rice 3 K genomes panel (https://snp-seek.irri.org/phenotype_dict.pdf) [42,43]. Plant height (PLHT) was defined as the distance from the base of the stem to the tip of the flag leaf. Leaf water potential (LWP, Ψ_{Leaf}) was directly measured in the field, consistently using the second fully-expanded leaf after the flag leaf for each genotype. Ψ_{Leaf} was determined after pressurizing the leaf with compressed N_2 at mid-day using a 3000HGBL Plant Water Status Console (SoilMoisture Equipment Corp.) and recording the minimum pressure at which outward sap flux could be observed. The same leaf was used to measure leaf area (LA), leaf length (LLT), and leaf width (LWD) with a leaf area meter (Li3100C; LI-COR, Lincoln, NE, USA), and leaf dry weight (LDW), which were further used to calculate the specific leaf area (SLA; leaf area / leaf dry weight).

Leaf rolling (LR) was scored by recording visual SES scores [44] in 2017 DS, and an HTP method to determine LR was calculated from the difference in NDVI values (ΔNDVI) as previously conducted [45]. Higher positive SES scores reflect a greater degree of leaf rolling, whereas a negative value of LR reflects the upward curling of the leaf. Additionally, the ΔNDVI (NDVI before applying stress – NDVI value after the stress treatment) obtained from drone multispectral images on 81 DAS vs. 84 DAS in 2017DS and 79 DAS vs. 112 DAS in 2019 DS, was taken as a proxy for LR in both seasons.

2.2.3. Leaf gas-exchange measurement of instantaneous photosynthesis

Leaf gas exchange measurements were conducted using Li-6400XT infrared gas exchange analyzers (LI-COR Biosciences, Lincoln, NE, USA) fitted with a standard 2 × 3 cm leaf chamber and 6400–02 B light source at a constant airflow rate of 400 μmol s^{-1}, leaf temperature of 30°C, leaf-to-air vapor deficit between 1.0 and 1.5 kPa and relative humidity of 60–65%. Data was recorded in the field in situ between 8AM to 1PM. Instantaneous photosynthesis rate (*A* or A_{net}) was recorded from the mid-portion of the leaf blade, separately on three fully expanded leaves per plant after a steady state was reached. Ten Li-6400 machines were used simultaneously in the field to complete this large number of measurements within a short time. Each Li-6400XT machine was calibrated before using, and the data was cross-checked by measuring the check varieties before, in-between and at the end of measurements each day. The gas-exchange measurements were completed within a window of 7 days. Recording the instantaneous photosynthetic rate of genotypes included net carbon assimilation per unit leaf area (*A or* A_{net}), transpiration per unit leaf area (*E*), stomatal conductance (g_s), and intercellular CO_2 (*Ci*). Instantaneous water use efficiency (WUE or WUE_i) was derived by dividing *A* by *E*. Additional parameters including *A*/ g_s, *E*/ g_s, and *Ci*/ g_s were evaluated to determine the fraction of the total stomatal conductance utilized for *A*, *E* or *Ci*. Leaf thickness (LT) was determined by dividing LA by SLA and was used to calculate the parameter A×LT, which was considered to represent assimilation per cubic leaf volumetric space.

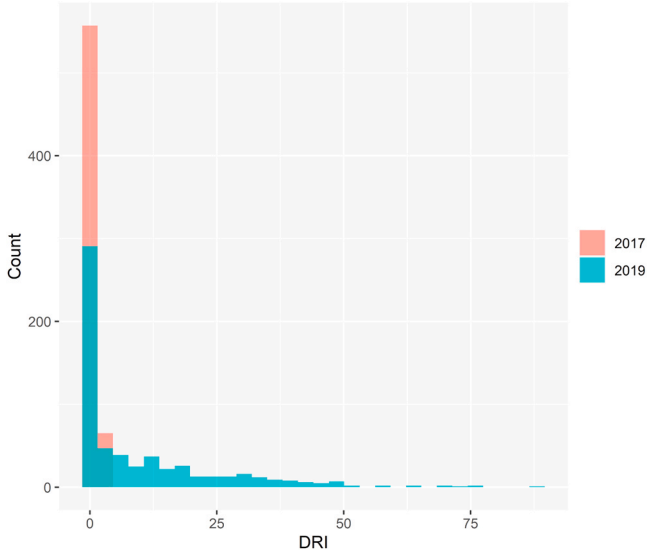

Fig. 2. Range of drought response index (DRI) values in 2017DS and 2019DS DS. N = 623 in 2017DS and N = 576 in 2019DS.

2.2.4. Data analysis

The values of least squared means for each trait were calculated for each genotype, with genotype as a random factor using the 'lmer' function in R version 4.2.1 (R project, www.rproject) [46] using linear mixed model of $y = x\beta + Zg + \varepsilon$, where, y = observed phenotypic value, $x\beta$ = fixed effect (replication), Zg = random effect of genotype, ε = random residual error. Outlier values above the 95th and below the 5th percentile with unexpected values for leaf measurements and missing values were excluded prior to use in correlation and GWAS analyses. Out of the 968 and 578 genotypes planted in 2017DS and 2019DS, 623 and 391 were used respectively after data cleaning to include a full set of all traits for the correlation analyses. Broad sense heritability of traits (H^2) was calculated as $H^2 = (V_G / V_G + V_E/r)$, where V_G = genetic variance, V_E = environmental variance and r = replication.

All traits were evaluated in both well-watered (WW) and managed drought stress (MDS) conditions to further analyse the drought response in terms of the differences (Delta, Δ, prefixed with "d" with traits in the figures) in their values in the WW and MDS treatments. PCA and correlations were performed using 'prcomp' and 'corrplot' functions in R.

2.2.5. GWAS study

Genome-wide association study was conducted using the 3000 Rice Genome 1 million Genome-wide association study single nucleotide polymorphism data [39,47]. In 2017DS, 592 genotypes were included in the GWAS for DRI, HI, SLA, WUE and CT while in 2019DS 572 genotypes were included in the GWAS for DRI, and 376 genotypes were used in the GWAS for SLA, WUE, and CT. We could include more genotypes in the GWAS study of DRI compared to other traits as the set of grain weight data was available for a greater number of genotypes in both seasons.

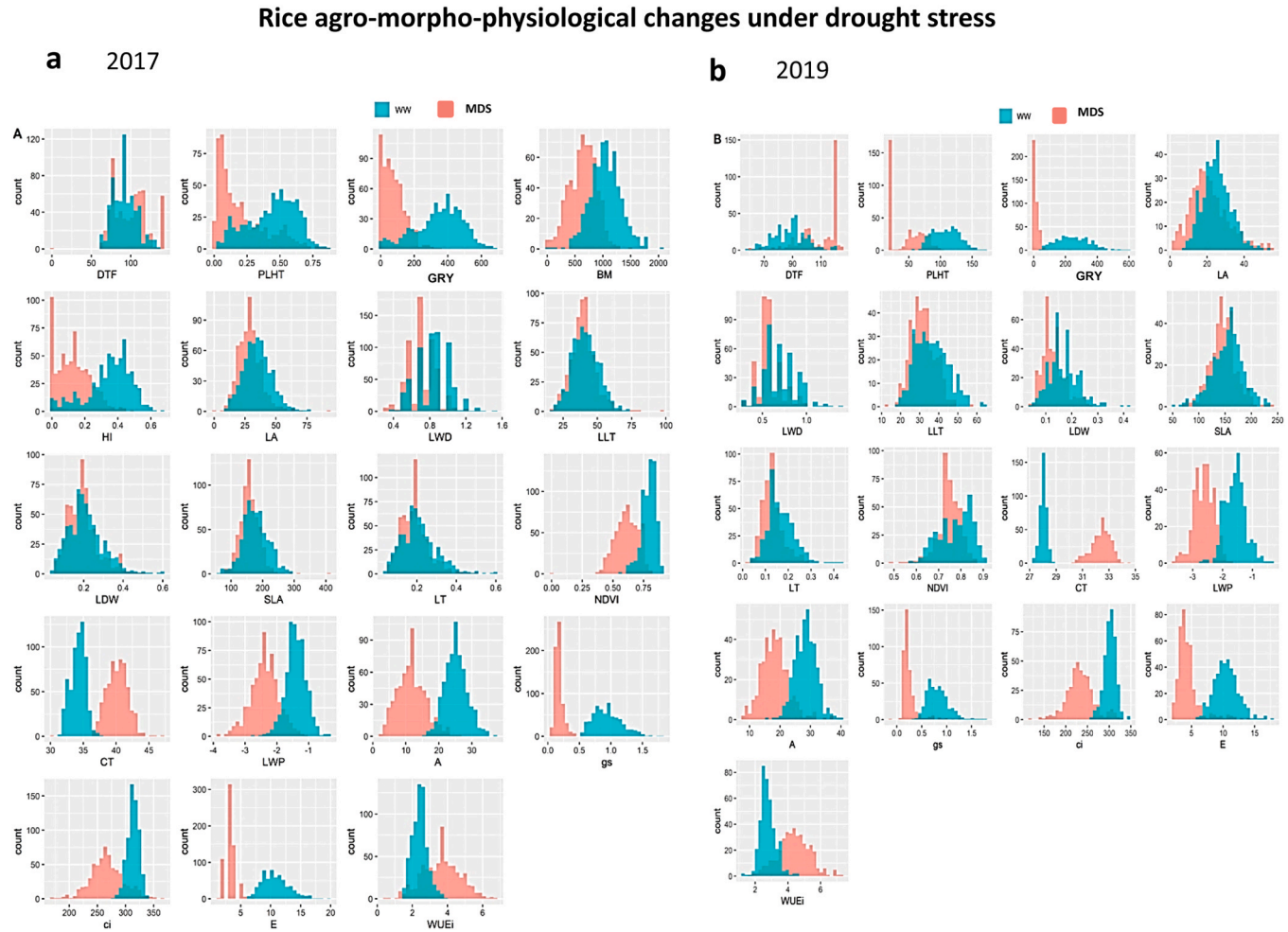

Fig. 3. Agro-morphological and functional responses of rice genotypes under WW and MDS in (a) 2017DS (b) 2019DS. Trait abbreviations and units are given in Table 1. N = 623 for 2017DS, N = 391 for 2019DS.

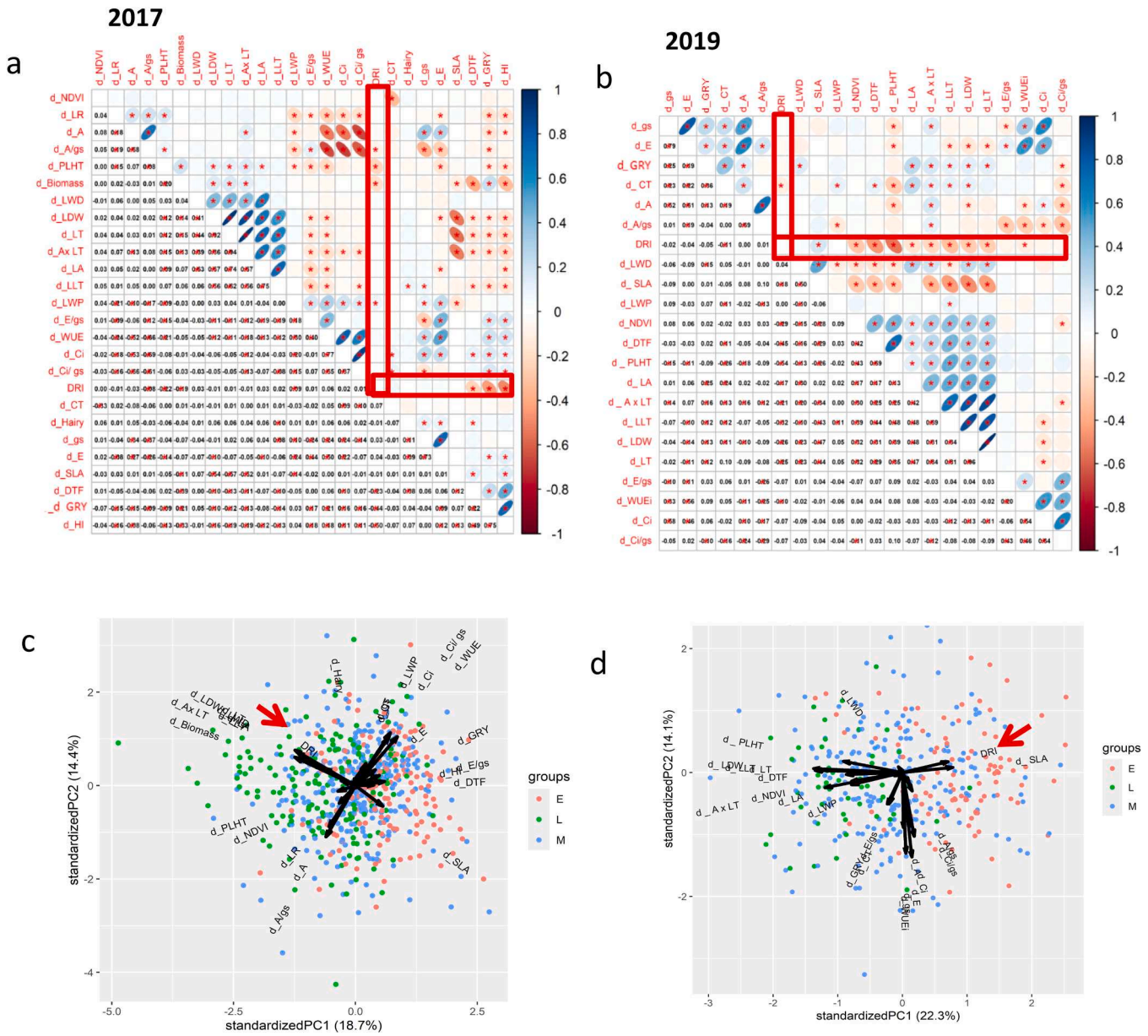

Fig. 4. Association of traits in terms of their drought-induced changes. Spearman's correlation matrices of drought response (Δ) for each trait in (a) 2017 DS and (b) 2019 DS. The traits are hierarchically clustered according to their degree of correlation. The blue ellipses above the upper diagonal show positive interactions while the red ellipses show negative correlations among the traits. Values below the lower diagonal consist of the respective R^2 values. '*' designates significant ($P < 0.05$) correlations. The red rectangles show correlations of traits with DRI (drought response index). The trait abbreviations are given in Table 1. N = 623 for A and N = 391 for B. c) PCA biplots of traits according to their response in field drought stress (Δ) in 2017 DS and d) 2019 DS. Arrows represent the position of DRI. E = early maturing, M= medium maturity and L = late maturity genotypes.

The SNP data was filtered using PLINK 1.90b3b [48] based on minor allele frequency (>0.05), and the linkage disequilibrium (LD) pruned data set was generated by the 'indep-pairwise' command with window size = 2 kb and $r^2 = 0.85$. The ped and map files generated by PLINK were then converted to HapMap files through Tassel 5.0 [49]. Finally, association tests were run separately for the drought dataset of DRI, HI, SLA, WUE and CT and analyzed using a linear mixed-model implemented in efficient mixed-model association (EMMA) by the R package of the Genome Association and Prediction Integrated Tool Package (GAPIT) [50,51]. Original values of DRI were converted to proportionate positive values and then log transformed before using for GWAS (Table S7, Table S9 [52]). The genome-wide GWAS significance threshold level was determined using the Bonferroni formula by dividing the standard significance level (alpha =0.05) by the effective number of independent tests [53] that corresponded to -log10(p)= 6.3. GWAS peaks were determined either using a threshold of -log10(p)= 5 or a less strict threshold of -log(p) = 4 which are widely used in rice GWAS studies, especially for the rice 3 K panel [19,29,54]. We interpret such peaks as having suggestive evidence and requiring additional follow-up work; these suggestive threshold lines are indicated on the Manhattan plots reported here.

Distribution of SNPs in a 100 Kb genomic region at specific QTLs was plotted using GoBii Haplotype Visualization Tool (https://haplotool-docs.readthedocs.io) [18]. Favorable haplotypes were identified by replotting the SNP pattern in a smaller genomic window of 30 kb surrounding the identified QTL to compare a smaller subset of two extreme groups of genotypes representing the 25 highest and 25 lowest DRI values.

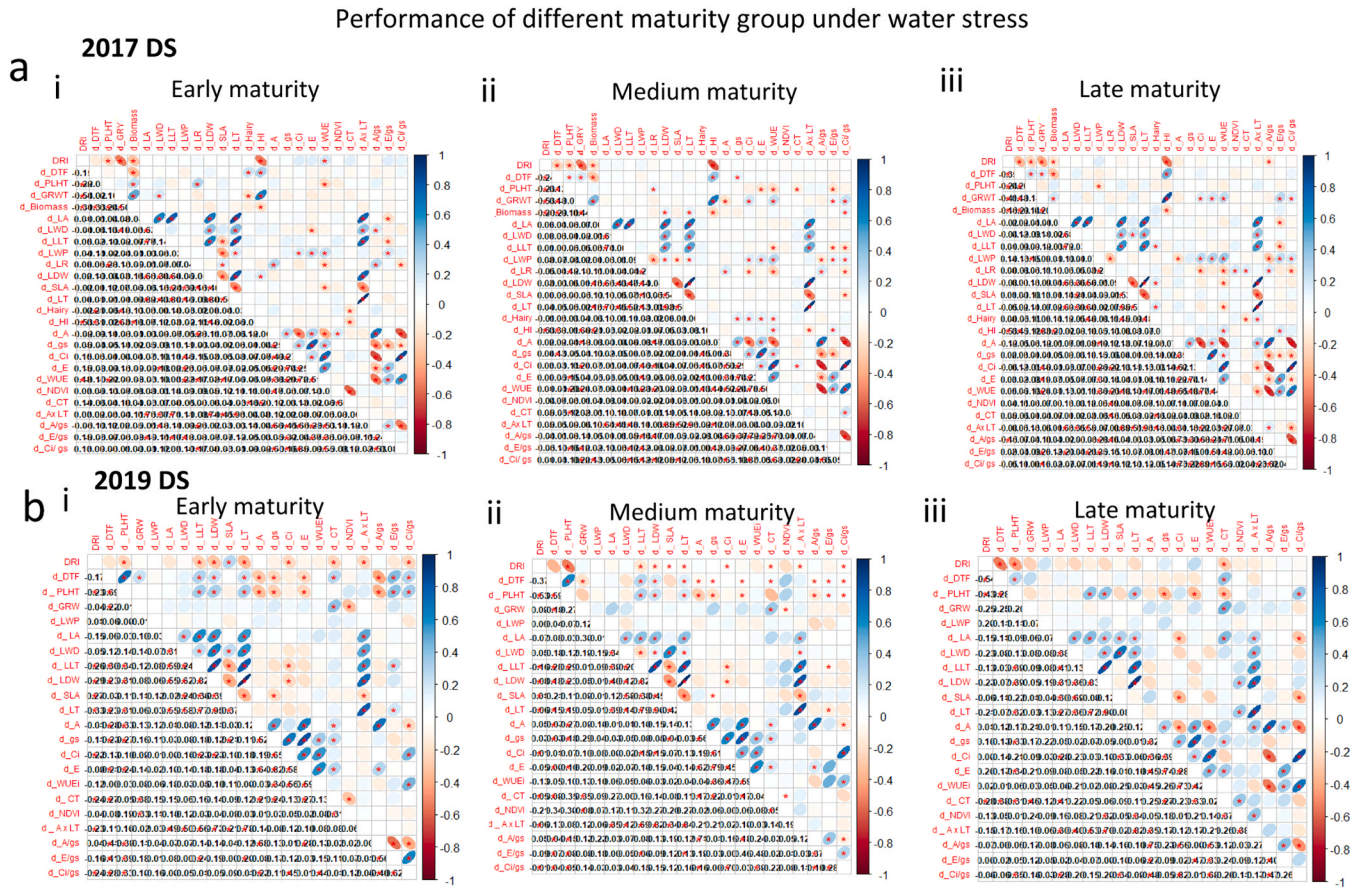

Fig. 5. Drought induced trait to trait correlation patterns in different maturity groups. a) Spearman's correlations matrix of drought responses (Δ) for each trait in 2017DS (early i, medium ii, and late iii group) and b) 2019DS (early i, medium ii and late iii group). The blue ellipses in the upper diagonal show positive interactions while the red ellipses show the negative correlations among the traits. The lower diagonal consists of the respective R^2 values. '*' designates significant ($P < 0.05$) correlations. The trait abbreviations are given in Table 1. N = 153 for early, 292 for medium, and 177 for late maturity genotypes in 2017DS and 105 early, 231 medium, and 54 late maturity genotypes in 2019DS.

2.2.6. Candidate gene analysis and gene interaction prediction

Candidate genes were identified using SNP seek (https://snp-seek.irri.org/) and MSU genome browser (http://rice.uga.edu/). The gene ontology and gene function was determined using the Rice Genome Annotation Project (RGAP). Indica-genome specific IR64 lifted over gene list (Table S10), gene function, intra- and inter-QTL genetic networks were analyzed using RicePilaf [55]. Gene interactions were determined by adding query protein sequence information in the STRING database version 12.0 [56]. Expression profiles of drought-response of candidate genes were acquired from the NetREx public database to search network-based rice expression analysis for abiotic stress tolerance [57].

3. Results

3.1. Drought delayed flowering time, reduced grain yield and photosynthetic performance, and altered leaf morphology in the 3 K indica panel

3.1.1. Leaf attributes in WW treatment

A large degree of genetic variation was observed in leaf traits and agronomic traits in the 968 indica genotypes that were planted in 2017DS, of which 578 genotypes were planted again in 2019DS. Representative images of the field and temporal variation in CT are shown in Fig. 1. Although the drought treatment was effective in both seasons as evidenced by raised canopy temperatures (Fig. 1b), drier conditions were experienced in 2019DS based on weather data of the two seasons (Table S2 and Table S3). The range of DTF values in the WW treatment varied between 60 and 137 DAS in the two seasons, based on which the genotypes were classified into three maturity groups: early (<80 DTF), medium (80–100 DTF) and late (>100 DTF). The range, average values, and the genetic diversity of all traits are presented in Table S5 collectively and separately for the different maturity groups to explore any unique characteristics present in any of the maturity groups. Grain yield (GRY) in the WW treatment ranged from 4.69 to 682.6 g m^{-2} in 2017DS and 32.18 – 599.5 g m^{-2} in 2019DS, which averaged ~350 g m^{-2} and ~250 g m^{-2} in 2017DS and 2019DS, respectively. Excessively low GRY of some genotypes under well-watered conditions was probably due to poor adaptation to the conditions in the Philippines. PLHT in the WW condition ranged from 45.3 to 170.3 cm in the two seasons. The LA varied from 8.93 to 78.1 cm^2 in 2017DS and 7.46 – 53.1 cm^2 in 2019DS. LWD varied 5-fold from 0.3 to 1.5 cm in both seasons, LLT varied ~4-fold from 17.4 to 74 cm, and LDW varied from 0.04 to 0.60 g, whereas SLA varied from 50.3 to 284.4 cm^2 g^{-1} (Table S5). Among leaf functional traits, LWP varied > 8 fold, ranging from −0.32 (MPa) to −2.7 (MPa); photosynthetic trait *A* varied > 2.5 fold, ranging from 15.3 to 40.2 μmol CO_2 / m^2 / s; g_s ranged from 0.3 to 1.8 μmol H_2O / m^2 / s; *E* varied around 3.3 fold, ranging from 5.79 to 19.5 mmol H_2O/ m^2 /s; and the *Ci* varied almost 1.5 fold among genotypes, ranging from 259.4 to 348.3 ppm CO_2. The WUE, which is the ratio of *A*/*E*, varied 3.5 times, ranging from 1.31 to 4.61 mmol H_2O / m^2 /s^1.

Notably, plant vigor was observed to increase with longer maturity as evidenced by the increasing PLHT, BM, LLT, and LDW, while SLA

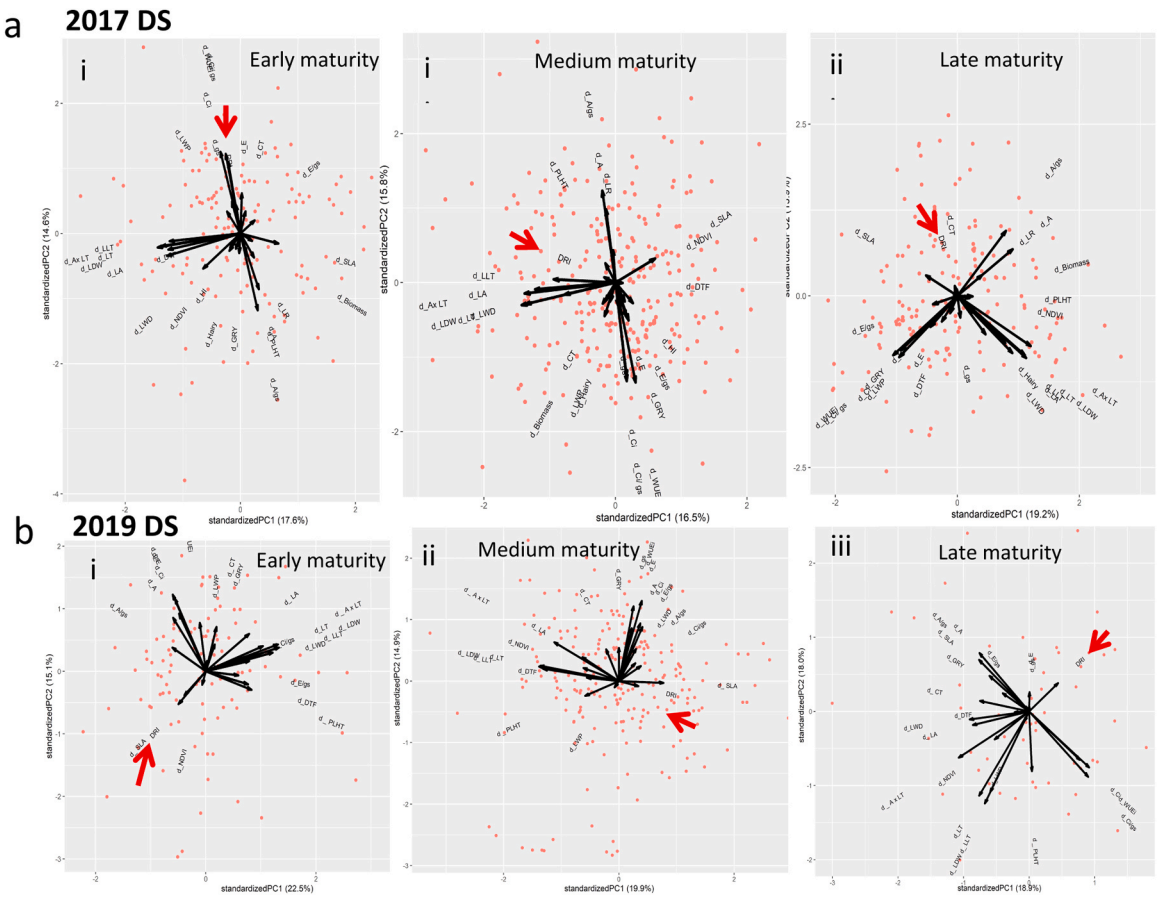

Fig. 6. PCA biplots of traits according to their responses to field drought stress (Δ) in a) 2017DS (early i, medium ii, and late iii groups) and b) 2019DS (early i, medium ii, and late iii groups). Arrows represent the position of DRI. E = early maturing, M= medium maturity and L = late maturity genotypes. The trait abbreviations are given in Table 1. n = 153 for early, 292 for medium, and 177 for late maturity genotypes in 2017DS and 105 early, 231 medium, and 54 late maturity genotypes in 2019DS.

decreased. However, in terms of water use, a slight increasing trend in WUE and decrease in *E* were observed across the maturity groups from early to medium to late flowering groups. The declining trend in SLA alternatively suggested an increased leaf thickness in medium and long duration genotypes. However, these trends did not translate to increased GRY in longer duration genotypes (Table S5).

3.1.2. Drought-driven shift in agro-morpho-physiological attributes in the 3 K indica panel

The dry-down during MDS treatment resulted in a 15% and 30% reduction in soil moisture contents in 2017DS and 2019DS (Fig. S1), representing moderate and severe drought stress, respectively. In this study, drought tolerance of each genotype was primarily defined by the drought response index (DRI), which is a comparison of the actual and predicted grain yield under drought (GRY_MDS), as determined by normalizing the yield under well-watered conditions (GRY_WW) by flowering time (DTF_WW) (Fig. 2). Genotypic responses under drought for the agronomic, HTP, leaf morphology, and functional traits were determined by the differences (Δs) of the trait values obtained during WW vs. those obtained in the MDS treatments and represented by the overall shift in the peak of that trait value under MDS conditions (Fig. 3). In both seasons, the time to flowering was delayed due to MDS treatment and growth reduction was prominent, as evidenced by loss of biomass and reduction in LA, LLT, LWD, LDW, SLA, LT, and NDVI. The decline in leaf functional parameters under MDS was evidenced by reduced LWP, HI, *A, E,* g_s and in *Ci*, the total CO_2 available for photosynthesis in the intercellular spaces (Fig. 3). In contrast, an increase in CT and WUE under MDS was evident in both seasons (Fig. 3).

The relative lack of flowering delay in 2017 under MDS was probably due to the relatively mild drought stress in the field as compared to the 2019 MDS treatment. However, the drought response was visible as evidenced by the loss in the GRY in both seasons, which was reduced by 77% and 94% respectively in 2017DS and 2019DS. We observed a greater reduction in the values of leaf morphological traits in the 2019DS MDS treatment, including a 12% reduction in LLT and 28% reduction in LWD as compared to only 3.8% and 14.8%, respectively in the 2017DS MDS treatment. Similarly, we noticed a greater reduction in LDW (22%) and SLA (8%) in 2019DS compared to the 8% and 5% reduction in 2017DS by the MDS treatment. Likewise, a profound drought effect was observed on the rice leaf functional traits compared to the WW treatment, including a 70 and 65% reduction in LWP in 2017DS and 2019DS, along with a 35–56% reduction in net carbon assimilation rate (*A*), 69–81% reduction in g_s, 14–22% reduction in *Ci*, and 57–69% reduction in *E* on average. WUE was ~ 50% higher on average under MDS compared to WW in both seasons. At the time of gas exchange and leaf measurements, canopy temperature was 17% and 15% warmer in MDS than in the WW treatment in 2017DS and 2019DS, respectively (Table S5).

3.2. Correlations among leaf morphological-functional traits in well-watered vs. managed drought stress treatments

Two major groups of correlations were prominent in the WW correlation matrix (Fig. S2 a, b) that reflect the initial relations between traits in a favorable environment; one was within different leaf morphological components, and the second was among the leaf

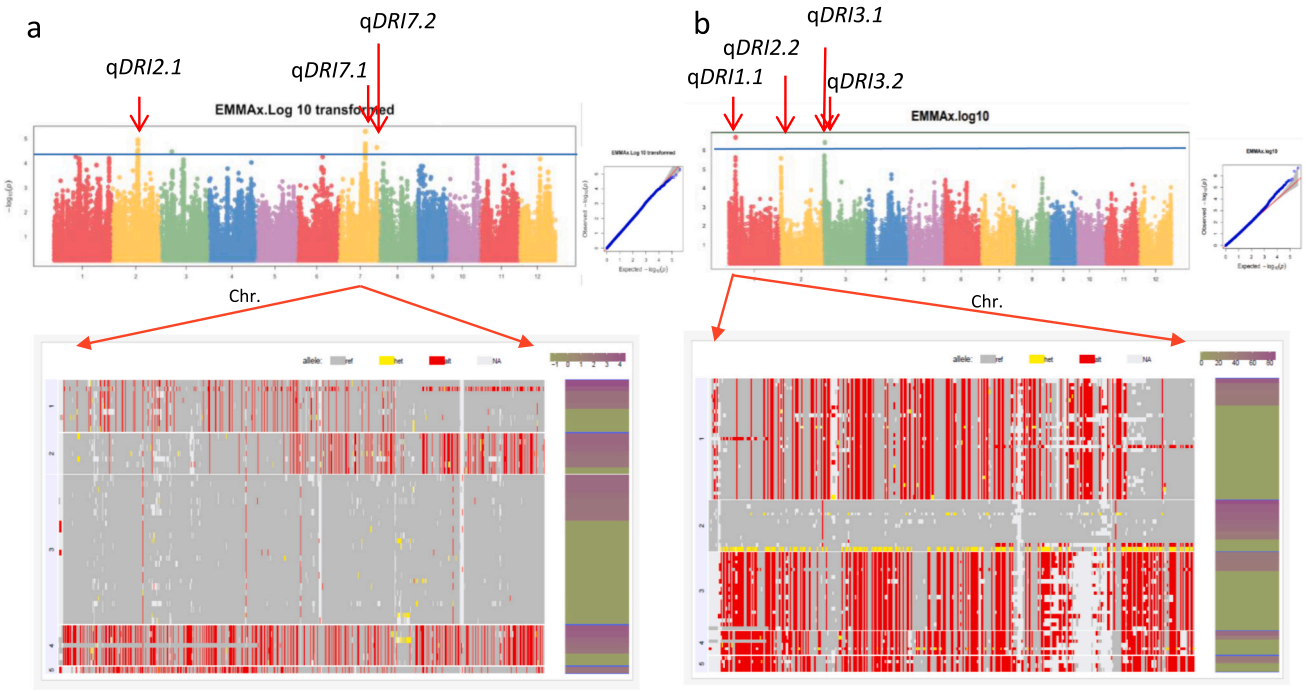

Fig. 7. Genome-wide SNPs association for drought response index (DRI) in (a) 2017DS and in (b) 2019DS including Manhattan plots and quantile-quantile plots at right (top), and a zoomed window of ±30 Kb genomic region of qDRI7.1 (a) and qDRI1.1 (b) below showing differences in SNP distributions among haplotypes by analysing genotypes with highest and lowest DRI values. The blue solid line in the Manhattan plot is the line of significant marker-trait association. GWAS was conducted on 592 genotypes with 410438 SNPs for the 2017DS data and on 572 genotypes with 417155 SNPs for 2019DS data.

functional components. We observed positive correlations of BM with leaf morphological traits (LLT, LA, LT, LDW) and photosynthetic traits (A×LT); while the relations of HI with these traits were negative (Fig S2a). However, there were noticeable correlations found linking the morphological and functional traits as well: the leaf photosynthetic trait A×LT showed significant positive correlations with leaf morphological traits LLT, LWD, LA, and LDW across two seasons (Fig S2). In contrast, photosynthetic trait E/g_s was negatively associated with these leaf morphological traits. Interestingly, in the 2019DS WW treatment, the LWD, SLA, and LWP showed significant positive correlations when compared to DRI; while the relation of LLT, LDW and LT, NDVI, and DTF were negatively correlated with DRI (Fig. S2b). However, no significant correlations between DRI and leaf traits were identified in the WW treatment of 2017DS.

The well-scattered positioning of the traits in the PCA biplot under WW conditions (Fig. S3) suggested an initial well-balanced contribution of the measured agronomic, morphological, and functional parameters, whereas the drought effect on these traits was reflected by a distortion of similar distributions in the MDS biplots replaced by closer associations between specific traits (Fig. S5 vs. Fig. S3). We found that LWP under MDS was positively related to DRI in both seasons (Fig. S4a, b). In 2017 under MDS, the higher DRI was mostly influenced by high HI (Fig. S4 a, Fig. S5 a), whereas more leaf traits were found to be correlated with DRI in the 2019 MDS biplot. DRI remained positively grouped together with leaf morphological traits LDW, LT, LA, and LLT in 2019 MDS with a close association of A×LT while showing a negative relationship with WUE (Fig. S4b).

The performance differences of traits in the WW vs. MDS treatments (represented as the delta (Δ), prefixed with "d" with trait abbreviations in the figures) showed negative correlations of DRI with ΔGRY (R^2 = −0.4, $P < 0.05$) and ΔHI (R^2 = −0.5, $P < 0.05$), ΔDTF, ΔBiomass, ΔPLHT, $\Delta A/g_s$ in 2017DS (Fig. 4a). This resulted in close associations of ΔLWD, ΔLA, ΔNDVI, ΔA×LT and ΔBM with DRI in the 2017DS PCA biplot (Fig. 4c). In 2019DS, DRI showed significant negative correlations with ΔCT (R^2 = - 0.12, $P < 0.05$), ΔWUE_i (R^2 = - 0.09, $P < 0.05$), ΔLA (R^2 = - 0.2, $P < 0.05$), ΔA×LT (R^2 = - 0.23, $P < 0.05$), ΔLLT (R^2 = - 0.36, $P < 0.05$), ΔLDW (R^2= - 0.30, $P < 0.05$), ΔLT (R^2 = - 0.29, $P < 0.05$), ΔNDVI (R^2 = - 0.37, $P < 0.05$), ΔDTF (R^2 = - 0.64, $P < 0.05$) and ΔPLHT (R^2 = - 0.60, $P < 0.05$) (Fig. 4b), suggesting retention of initial biomass and maintenance of lower canopy temperature reflecting better drought tolerance in terms of yield. In contrast, DRI showed a significant positive correlation with ΔSLA (R^2 = 0.2, $P < 0.05$) in 2019DS (Fig. 4d), suggesting a possible leaf morphological adjustmentto mitigate the effects of severe drought stress.

Among the three different maturity groups (early, medium and late), the pattern of correlations of leaf traits with DRI remained similar, although there were differences in their strength of associations (Fig. 5a, b). In the PCA biplots, fewer leaf traits were grouped together with DRI in the late maturity group in both seasons (Fig. 6a, b, iii). The association of ΔSLA with DRI in both early and medium maturity groups in 2019DS added confidence to the assumption that a greater reduction in SLA under drought was associated with increased drought tolerance (Fig. 6b panels i and ii).

3.3. Identification of drought associated genomic loci

Genome wide marker-trait association was performed for DRI, SLA_MDS, WUE_MDS and CT_MDS in 2017DS and 2019DS, and for HI_MDS in 2017DS. These traits were included in the GWAS analysis as those were the leaf agronomic, morphological and photosynthetic traits recurrently associated with DRI across different correlation analyses with moderate H^2 values (broad sense H^2 of GRY = 30–33%, HI = 33%, SLA= 30–31%, WUE = 14 – 30%, CT = 20 – 21%). The detailed genetic structure of the population is given in Fig. S6. Genome wide association studies (GWAS) identified 7 major QTLs for DRI: 4 QTLs based on a significant cutoff value of $-\log_{10}(P) > 5$ in 2019DS and 3 QTLs based on a significant cutoff at $-\log_{10}(P) > 4.5$ in 2017DS (Fig. 7). The DRI QTLs were distributed as follows: one QTL on chr 1 (qDRI1.1), two on chr 2 (qDRI2.1, qDRI2.2), two on chr 3 (qDRI3.1, qDRI3.2), and two on chr 7 (qDRI7.1, qDRI7.2) (Fig. 7a, b). Similarly, one QTL on chr 12 at

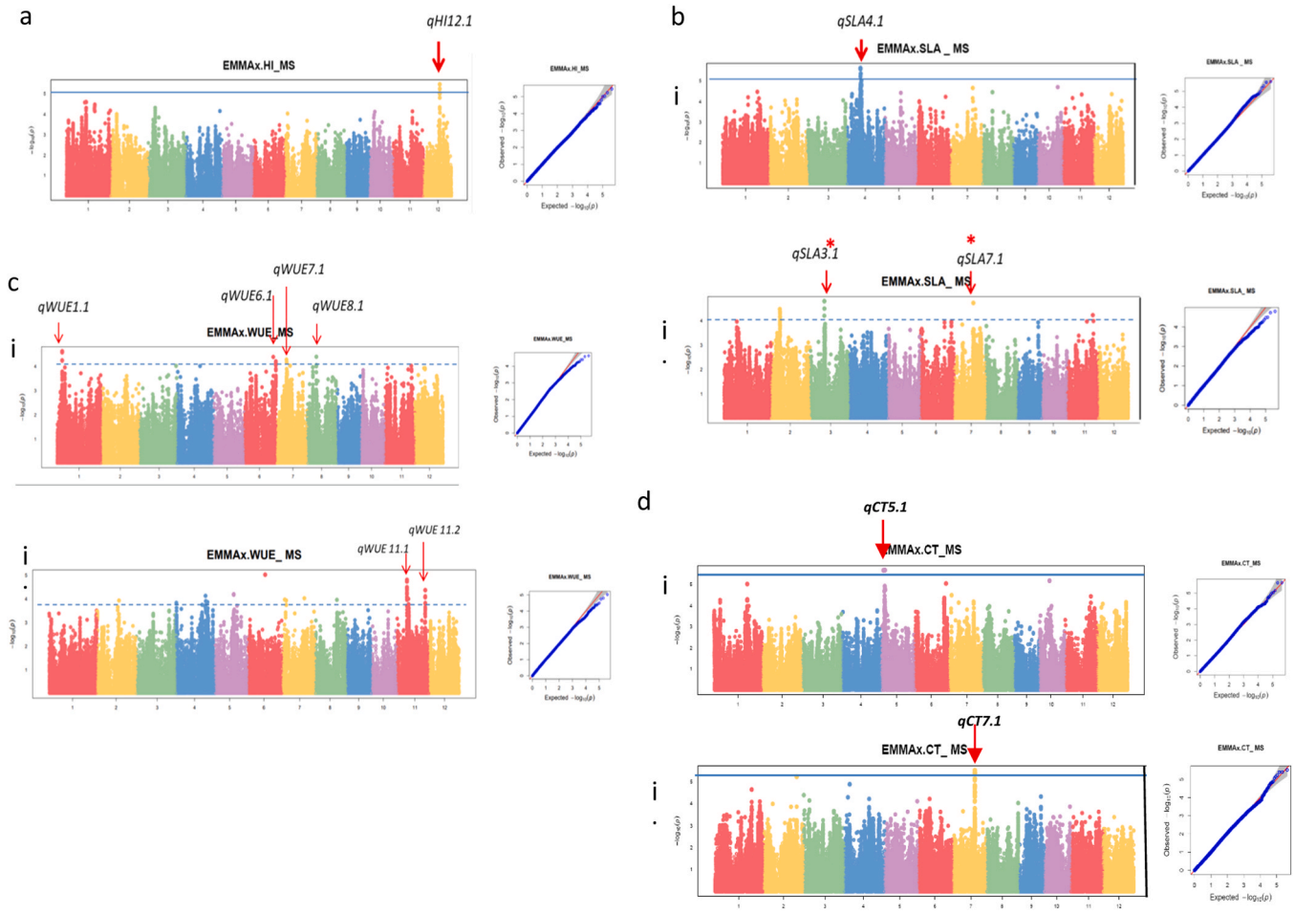

Fig. 8. Manhattan plots of genome–wide marker-trait association for (a) HI, (b) SLA, (c) WUE, and (d) CT in (i)2017DS and in (ii) 2019DS under MDS (ii). The panels on the right shows the respective quantile-quantile plots. Blue solid lines in the Manhattan plots indicate the threshold considered for significant marker – trait associations. GWAS was conducted on 596 genotypes with 448065 SNPs for HI, SLA and WUE in 2017DS. In 2019DS, GWAS was conducted on 376 genotypes with 438039 SNPs. For SLA in 2019DS, the SNP peak marked with red stars is discussed in detail.

$-\log_{10}(P) > 5$ was identified for HI from 2017 MDS (Fig. 8a). Three QTLs were identified for SLA_MDS (Fig. 8b); one on chr 4 at $-\log_{10}(P) > 5$ in 2017DS, and two others each on chr 3 and chr 7 at $-\log_{10}(P) > 4$ in 2019DS. Six QTLs were identified for WUE_MDS at a significant cutoff value of $-\log_{10}(P) > 4$. Four of the QTLs were identified on chr 1, 6, 7, 8 in 2017DS, and two QTLs were identified on chr 11 in 2019DS (Fig. 8c). Two sharp peaks, qCT5.1 and qCT7.1 at $-\log_{10}(P) > 5$ were identified for CT under MDS (Fig. 8d).

We looked for candidate genes associated with the respective traits within 100 kb vicinity of the identified peak SNP locus. The SNP distribution pattern for two QTLs is given in Fig. S7 to show evidence of LD and different haplotypes due to genetic recombination. Gene lists within a 100bb region of the identified QTLs were extracted using Rice-Pilaf (Table S10). *In silico* analysis found a total of 54 genes within the 100 kb genomic regions of the identified DRI QTLs (Table 2, detailed information about the QTLs is in Table S11). Among these, a 1,4 glucan–-branching enzyme (LOC_Os02g32660.1), a HSF-type DNA binding domain protein (LOC_Os02g32590.1), a DEAD-box helicase (LOC_Os07g46580.1), a SNF2 family N terminal domain containing protein (LOC_Os07g46590.1), a WD repeat-containing protein (LOC_Os07g46620.1), and, notably, an early response to dehydrin gene (LOC_Os07g46670.2) were important candidate genes identified from the 2017DS DRI GWAS. Similarly, an aquaporin protein (LOC_Os01g10600.1), a wall associated kinase protein, a glyceraldehyde-3 phosphate dehydrogenase (LOC_Os03g03720.1), a calcium/calmodulin dependent protein (LOC_Os03g02980.1), and a flavonol synthase (LOC_Os03g03034.1) were notable candidate genes identified for DRI in 2019DS.

QTL qHI12.1 possessed precisely two transferase family protein genes in the 100 kb genomic region (Table 3). Of the 12 candidate genes associated with SLA under MDS, some interesting candidate genes noted were the short chain dehydrogenase – reductase type of genes which were recurrently identified for DRI and SLA in 2017DS. A transcription factor F-box domain containing protein (LOC_Os03g22990.1), a zinc finger, C3HC4 type domain containing protein (LOC_Os03g22830.2), and an actin-depolymerizing factor (LOC_Os07g30090.2) were identified which might play a role in leaf development and possibly regulate leaf thickness under drought. GWAS peaks for WUE were only identified using lower cutoff values ($-\log_{10}(P) > 4$). Genes including the Myb transcription factor (LOC_Os01g09640.1), F-box domain containing protein (LOC_Os11g16280.1), and a transporter family protein (LOC_Os11g42430.1), presented in the WUE QTL regions, might play crucial roles in determining WUE under drought stress. A total of 14 genes were present in the QTL regions identified for CT (Table 3), of which the proline synthetase co-transcribed bacterial homolog protein, putative, expressed (LOC_Os05g05740.1) and UDP-glucoronosyl/UDP-glucosyl transferase, putative, expressed (LOC_Os07g32060.1) might be good candidate genes to explore further as they are known to provide heat tolerance to plants by UV protection and were highly expressed in seedling in cold stress [58]. Interestingly, region qCT7.1 coincides with the region qDRI7.1, and a co-expression analysis of both regions in Rice-Pilaf (https://ricepilaf.bioinfodlsu.com/, accessed on 21 June

Table 2
List of genes present in the 100 Kb window of the identified QTLs associated with DRI. Details of the QTLs identification parameters are given in Table S11.

QTL name	Candidate gene locus in the 100 kb window	Protein name
qDRI2.1	LOC_Os02g32660.1	1,4-alpha-glucan-branching enzyme, chloroplast precursor, putative, expressed
	LOC_Os02g32620.1	PAN domain-containing protein At5g03700 precursor, putative, expressed
	LOC_Os02g32610.2	protein kinase domain containing protein, expressed
	LOC_Os02g32590.1	HSF-type DNA-binding domain containing protein, expressed
	LOC_Os02g32570.1	SNF2 family N-terminal domain containing protein, expressed
qDRI7.1	LOC_Os07g32600.1	glucan endo-1,3-beta-glucosidase precursor, putative, expressed
	LOC_Os07g32620.1	anthocyanidin 5,3-O-glucosyltransferase, putative, expressed
	LOC_Os07g32630.1	UDP-glucoronosyl and UDP-glucosyl transferase domain containing protein, expressed
	LOC_Os07g32660.1	monocopper oxidase, putative, expressed
qDRI7.2	LOC_Os07g46580.1	DEAD-box ATP-dependent RNA helicase, putative, expressed
	LOC_Os07g46590.1	SNF2 family N-terminal domain containing protein, expressed
	LOC_Os07g46600.1	RNA pseudouridine synthase, putative, expressed
	LOC_Os07g46610.1	cis-zeatin O-glucosyltransferase, putative, expressed
	LOC_Os07g46620.1	WD repeat-containing protein 55, putative, expressed
	LOC_Os07g46630.1	AMP deaminase, putative, expressed
	LOC_Os07g46640.1	UDP-N-acetylglucosamine-dolichyl-phosphate N-acetylglucosaminephosphotransferase, putative, expressed
	LOC_Os07g46660.1	ubiquitin carboxyl-terminal hydrolase domain containing protein, expressed
	LOC_Os07g46670.2	early response to dehydration 15, putative, expressed
	LOC_Os07g46690.1	PHD-finger family protein, expressed
	LOC_Os07g46700.1	zinc finger, RING-type, putative, expressed
qDRI1.1	LOC_Os01g10600.1	aquaporin protein, putative, expressed
	LOC_Os01g10610.1	BES1/BZR1 homolog protein, putative, expressed
	LOC_Os01g10590.1	osFTL8 FT-Like8 homologous to Flowering Locus T gene; contains Pfam profile PF01161: Phosphatidylethanolamine-binding protein, expressed
	LOC_Os01g10580.1	B-box zinc finger family protein, putative, expressed
	LOC_Os01g10550.1	DEFL35 - Defensin and Defensin-like DEFL family, expressed
qDRI2.2	LOC_Os02g01980.1	GDSL-like lipase/acylhydrolase, putative, expressed
	LOC_Os02g01990.1	CCT motif family protein, expressed
	LOC_Os02g02000.1	cytochrome P450, putative, expressed
	LOC_Os02g02020.1	pentatricopeptide, putative, expressed
	LOC_Os02g02040.1	protein kinase, putative, expressed
	LOC_Os02g02050.1	SNF2 family N-terminal domain containing protein, expressed
	LOC_Os02g02090.1	peptidyl-prolyl cis-trans isomerase, putative, expressed
	LOC_Os02g02110.1	Alg9-like mannosyltransferase protein, putative, expressed
	LOC_Os02g02120.1	OsWAK11 - OsWAK receptor-like protein kinase, expressed
	LOC_Os02g02130.1	ribosomal protein L37, putative, expressed
	LOC_Os02g02140.1	receptor protein kinase CLAVATA1 precursor, putative, expressed
qDRI3.1	LOC_Os03g03720.1	glyceraldehyde-3-phosphate dehydrogenase, putative, expressed
	LOC_Os03g03730.1	regulatory protein, putative, expressed
	LOC_Os03g03760.1	MYB family transcription factor, putative, expressed
	LOC_Os03g03790.1	AMP-binding domain containing protein, expressed
	LOC_Os03g03810.1	DEF8 - Defensin and Defensin-like DEFL family, expressed
	LOC_Os03g03820.1	adenylate kinase, putative, expressed
	LOC_Os03g03830.1	EF hand family protein, putative, expressed
	LOC_Os03g03850.1	GATA zinc finger domain containing protein, expressed
	LOC_Os03g03870.1	DNA-binding bromodomain-containing protein, putative, expressed
qDRI3.2	LOC_Os03g02920.1	peroxidase precursor, putative, expressed
	LOC_Os03g02939.1	peroxidase precursor, putative, expressed
	LOC_Os03g02960.1	nascent polypeptide-associated complex subunit alpha, putative, expressed
	LOC_Os03g02970.1	Dicer, putative, expressed
	LOC_Os03g02980.1	CAMK_CAMK_like_ULKh_APGy.1 - CAMK includes calcium/calmodulin dependent protein kinases, expressed
	LOC_Os03g03000.1	helix-loop-helix DNA-binding domain containing protein, expressed
	LOC_Os03g03020.1	L11 domain containing ribosomal protein, putative, expressed
	LOC_Os03g03034.1	flavonol synthase/flavanone 3-hydroxylase, putative, expressed
	LOC_Os03g03070.1	transcription factor, putative, expressed

2025) suggests that the mechanism of maintaining canopy temperature under drought to produce more grain may involve flavonol production (Fig. 9, with the list of co-expressed genes in Table S12) which may serve a role in photoprotection. Several of the genes in our identified QTL regions were found to be involved in potassium sensitivity, transmembrane transporter activity, flavonol biosynthesis, and microtubule movement that were confirmed by co-expression analysis in Rice-Pilaf (Fig. S12). A closer look at the genomic regions of regionqDRI7.1 and another important DRI QTL qDRI 1.1, revealed suggested haplotype 2 and 4 for qDRI7.1 and haplotype 2 for qDRI 1.1 to be favorable and would be worth exploring for potential use in breeding for high DRI (Fig. 7).

An overall analysis of the stress-induced expression profile of the identified candidate genes, extracted from public database NetRex (https://bioinf.iiit.ac.in/netrex/index.html., accessed on 18 June, 2025), indicated that 39 of the identified genes are differentially expressed under drought stress (Fig. 10a). Among the identified candidate genes, we considered dehydrin (LOC_Os07g46670.2), aquaporin (LOC_Os01g10600.1), and transferase (LOC_Os12g27254.1) to be of high interest, and, therefore, these were investigated further in terms of gene-network interactions (Fig. 10b). The early response dehydrin gene showed interactions with senescence domain – containing protein and peroxidase (Table S13) which are notable for their roles in drought tolerance. The aquaporin gene showed interactions with AAA domain containing proteins, glycerol-3 phosphate dehydrogenase, and other aquaporins as revealed by the network analysis (Table S14). Glycerol-3 phosphate dehydrogenase facilitates the conversion of glycerol-3-phosphate to dihydroxyacetone phosphate, which is a key energy generating component of the Calvin cycle, thereby suggesting a role of aquaporins in maintaining water balance during the photosynthetic light reaction. The transferase gene, which might facilitate assimilate mobilization to the grain under stress conditions, interacts with AAI domain containing proteins, cytochrome b5 heme-binding domain-containing protein, and a NADH-cytochrome b5 reductase belonging to

Table 3
List of genes present in the 100 kb window of the identified QTLs for HI, SLA, WUE and CT under MDS conditions. Details of the QTLs identification parameters are given in Table S11.

QTL name	Candidate gene locus in the 100 kb window	Protein name
qHI12.1	LOC_Os12g27210.1	expressed protein
	LOC_Os12g27254.1	transferase family protein, putative, expressed
	LOC_Os12g27220.1	transferase family protein, putative, expressed
qSLA4.1	LOC_Os04g22360.1	DUF647 domain containing protein, putative, expressed
	LOC_Os04g22380.1	short chain dehydrogenase/reductase protein, putative, expressed
	LOC_Os04g22390.1	short chain dehydrogenase/reductase protein, putative, expressed
qSLA3.1	LOC_Os03g22990.1	OsFBX84 - F-box domain containing protein, expressed
	LOC_Os03g22950.1	acyl carrier protein, putative, expressed
	LOC_Os03g22900.1	SNF2 family N-terminal domain containing protein, expressed
	LOC_Os03g22890.2	GTPase of unknown function domain containing protein, putative, expressed
	LOC_Os03g22880.1	nucleolar protein 5 A, putative, expressed
	LOC_Os03g22870.1	SAC3/GANP family protein, putative, expressed
	LOC_Os03g22830.2	zinc finger, C3HC4 type domain containing protein, expressed
qSLA7.1	LOC_Os07g30020.1	anthranilate phosphoribosyltransferase, putative, expressed
	LOC_Os07g30090.2	actin-depolymerizing factor, putative, expressed
	LOC_Os07g30100.1	RIN3, putative, expressed
qWUE1.1	LOC_Os01g09640.1	Myb transcription factor, putative, expressed
	LOC_Os01g09670.1	pollen-specific protein SF21, putative, expressed
	LOC_Os01g09700.1	aminotransferase, classes I and II, domain containing protein, expressed
	LOC_Os01g09740.1	F-box/LRR-repeat protein, putative, expressed
	LOC_Os01g09760.1	DIRP family protein, putative, expressed
	LOC_Os01g09790.1	IQ calmodulin-binding motif domain containing protein, expressed
qWUE8.1	LOC_Os08g14230.1	villin, putative, expressed
	LOC_Os08g14320.1	zinc finger, C3HC4 type domain containing protein, expressed
	LOC_Os08g14330.1	aldose 1-epimerase, putative, expressed
qWUE6.1	LOC_Os06g45940.1	potassium transporter, putative, expressed
	LOC_Os06g45950.1	OsSAUR25 - Auxin-responsive SAUR gene family member, expressed
	LOC_Os06g45960.1	cytochrome P450, putative, expressed
	LOC_Os06g45970.1	OsSAUR26 - Auxin-responsive SAUR gene family member, expressed
	LOC_Os06g45980.1	toprim domain-containing protein, putative, expressed
	LOC_Os06g45990.1	patellin-5, putative, expressed
	LOC_Os06g46000.1	tubulin/FtsZ domain containing protein, putative, expressed
	LOC_Os06g46030.1	DUF640 domain containing protein, putative, expressed
qWUE7.1	LOC_Os07g16130.1	acetyltransferase, GNAT family, putative, expressed
	LOC_Os07g16140.1	FAD binding protein, putative, expressed
	LOC_Os07g16224.1	piwi domain containing protein, putative, expressed
qWUE11.1	LOC_Os11g16260.1	laccase precursor protein, putative, expressed
	LOC_Os11g16280.1	F-box domain containing protein, expressed
	LOC_Os11g16290.1	NIN, putative, expressed
qWUE11.2	LOC_Os11g42420.1	nuclear pore protein 84/107 containing protein, expressed
	LOC_Os11g42430.1	transporter family protein, putative, expressed
	LOC_Os11g42450.1	leucine-rich repeat family protein, putative, expressed
	LOC_Os11g42480.1	transferase family domain containing protein, expressed
	LOC_Os11g42500.1	dirigent, putative, expressed
	LOC_Os11g42510.1	tyrosine aminotransferase, putative, expressed
	LOC_Os11g42550.1	dirigent, putative, expressed
	LOC_Os11g42580.1	Leucine Rich Repeat family protein, expressed
q*CT5.1*	LOC_Os05g05710.1	serine/threonine-protein phosphatase 2 A regulatory subunit B subunitgamma, putative, expressed
	LOC_Os05g05720.1	tetratricopeptide repeat domain containing protein, expressed
	LOC_Os05g05740.1	proline synthetase co-transcribed bacterial homolog protein, putative, expressed
	LOC_Os05g05780.1	chromatin-remodeling complex ATPase chain, putative, expressed
	LOC_Os05g05790.1	double-stranded RNA binding motif containing protein, expressed
	LOC_Os05g05800.1	OsFBL21 - F-box domain and LRR containing protein, expressed
	LOC_Os05g05810.1	DEAD-box ATP-dependent RNA helicase, putative, expressed
	LOC_Os05g05820.1	pro-resilin precursor, putative, expressed
	LOC_Os05g05830.1	bifunctional protein folD, putative, expressed
	LOC_Os05g05840.1	tRNA synthetase class II core domain containing protein, expressed
q*CT7.1*	LOC_Os07g32170.1	OsSPL13 - SBP-box gene family member, expressed
	LOC_Os07g32120.1	transcription initiation factor IIB, putative, expressed
	LOC_Os07g32080.1	transcription initiation factor IIB, putative, expressed
	LOC_Os07g32060.1	UDP-glucoronosyl/UDP-glucosyl transferase, putative, expressed

the flavoprotein pyridine nucleotide cytochrome reductase family (Table S15).

4. Discussion

While many previous studies have documented the drought response of leaf traits as an early sign of stress [9,23,59,60], leaf traits conferring tolerance to drought have not been consistently reported. Commonly, rice responds to drought stress initially by rolling leaves (LR) abaxially or adaxially [61,62], and this is often considered as the first visual symptom of drought response in rice plants. However, the genetic differences in rice leaf rolling under drought were reported to be mainly driven by leaf morphology and anatomy rather than productivity under drought [13]. Similarly, rice *ψLeaf* was reported to be insensitive to soil moisture deficit in a pot study with restricted root growth [63]. Thick leaves have also been observed to provide better drought tolerance [64]; this was attributed to increased cell wall thickness and cuticle layer of the laminar epidermal cells [65]. Drought tolerance breeding was reported to have selected longer rice flag leaves and lower stomatal densities [66,67]. Although rice leaves appear to be generally quite responsive to drought, few studies have linked those traits with grain yield production.

Currently, the yield of rice crops in drought prone areas stands very low and stagnant at an average maximum of ~3 t ha^{-1} [68] which is insufficient to meet agricultural demands. The responses of rice plants to drought have been documented as complex, involving various physiological, biochemical, and molecular changes that contribute to the resulting yield levels [69–72]. Exploring the indica rice 3 K panel, which

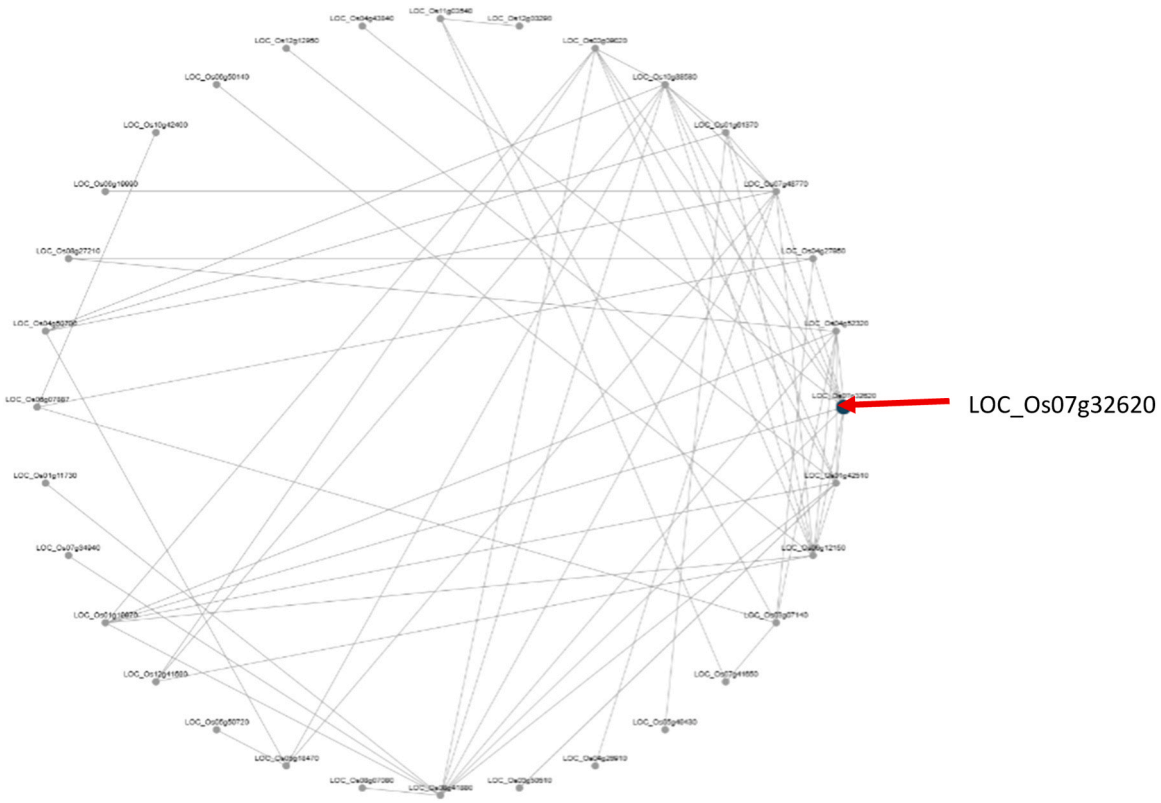

Fig. 9. Co-expression network analysis of the GWAS QTL qDRI7.1 (Chr07:19,050,099-19,150,099) and qCT7.1 (Chr07:19,433,074-19,533,074) using ClusterONE and RiceNet v. 2 in RicePilaf, showing a significantly enriched ($p < 0.05$) (Module 2577, adjusted p-value = 3.782527e-02) gene network that included LOC_Os07g32620 from the GWAS interval influencing biological pathways of flavonoid biosynthesis. The list of interactive genes is shown in Table S12. Locus LOC_Os07g32620 is particularly notable as the annotated gene UDP-Glucosyl transferase family protein is found to be present in both qDRI7.1 and qCT7.1, which may provide a genetic linkage for maintaining low canopy temperature and producing higher grain yield under drought.

is genetically diverse in its plant morphology, leaf, physiology, and agronomic traits, helped us define some of the fundamental drought-induced leaf structure/ function dynamics and highlighted morpho-functional attributes related to better yield under drought.

The introduction of several new "integrative" morpho-physiological parameters in our study – A×LT, A/g_s, E/ g_s, and Ci/g_s – helped us to overcome the limitation of linking single morphological traits to a single functional trait. Specifically, the leaf morphological character LT, calculated by dividing LA by SLA, was used as a proxy for leaf thickness, and the trait A×LT was considered to be the total assimilation per cubic cm of leaf tissue by adding a third dimension, the leaf thickness, to the assimilation value. Ci/g_s reflected the status of intercellular CO_2 concentration inside the leaf over stomatal conductance. Similarly, A/g_s and E/g_s were estimates of the proportion of the leaf stomatal conductance used either for CO_2 assimilation (A/g_s is also known as intrinsic water use efficiency) or for transpiration, respectively. Of these integrative traits, leaf morphological traits were found to be better associated with A×LT rather than with *A* or *E* alone (Fig. 4) due to a better estimate of the total amount of carbon being assimilated in a single leaf.

We observed seasonal variation in the responses of leaf traits due to differences in the level of drought exposure in two seasons. In 2019DS, drought severity drove more leaf trait associations with DRI, suggesting substantial leaf structural adjustments in response to increased level of stress in that season. Among the photosynthetic parameters, while the *A*, g_s and *Ci* declined under drought, WUE showed an increasing trend due to reduced *E* (Fig. 3), confirming the previous studies in rice [73–75].

One of our objectives for this study was to identify if there are any main physiological attributes that determine rice yield under drought. Among the physiological traits, the leaf water potential, ψ_{Leaf}, was previously reported to be an important drought response indicator [76–79] and it was found to be consistently positively correlated with DRI in both WW and MDS in 2019 (Fig. S2, Fig. S4). This confirmed that higher ψ_{Leaf} is indeed required for maintaining grain yield in rice under soil water deficit conditions. The positive correlations of ψ_{Leaf} with *E* under MDS (Fig.S4b) further confirmed that higher amounts of water in leaves under drought allows higher transpiration rates in rice, thereby facilitating sufficient levels of CO_2 inside leaves to maintain photosynthesis. Higher *E* eventually contributes to a cooler canopy temperature under drought as evidenced from the 2019DS dataset (Fig. S4b).

Next, we traced the association of leaf morphological traits to the functional traits to identify the key leaf traits stabilizing physiology and driving a higher grain yield in rice under drought. Generally, under water deficit, leaf rolling is prominent in rice while some varieties respond by leaf shrinkage to reduce evaporation and transpiration from the exposed leaf surface [80]. In our study, higher DRI correlated well with less fluctuations (Δ values) in leaf morphological and functional responses, except for SLA. The positive correlation of ΔSLA with DRI indicated that an increase in leaf thickness adjustments under drought was associated with higher grain yield. It is generally accepted that leaf thickness influences rice photosynthesis [81,82] and ψ_{Leaf} [83] under favorable conditions. Moreover, an increase in leaf thickness is known to be associated with an increased cuticle or wax layer on the surface [64, 65,84] that provides protection from desiccation. Some rice leaf traits, such as leaf hairs [22] and the leaf surface wax layer [85], have been reported to provide stability to leaf water status by limiting non-stomatal water loss during drought and would be interesting to characterize in the genotypes selected here. However, interestingly, we also found the SLA to be positively corelated with DRI under well-watered conditions, suggesting that genotypes with a broader leaf rather than a thicker leaf have a greater potential to alter drought

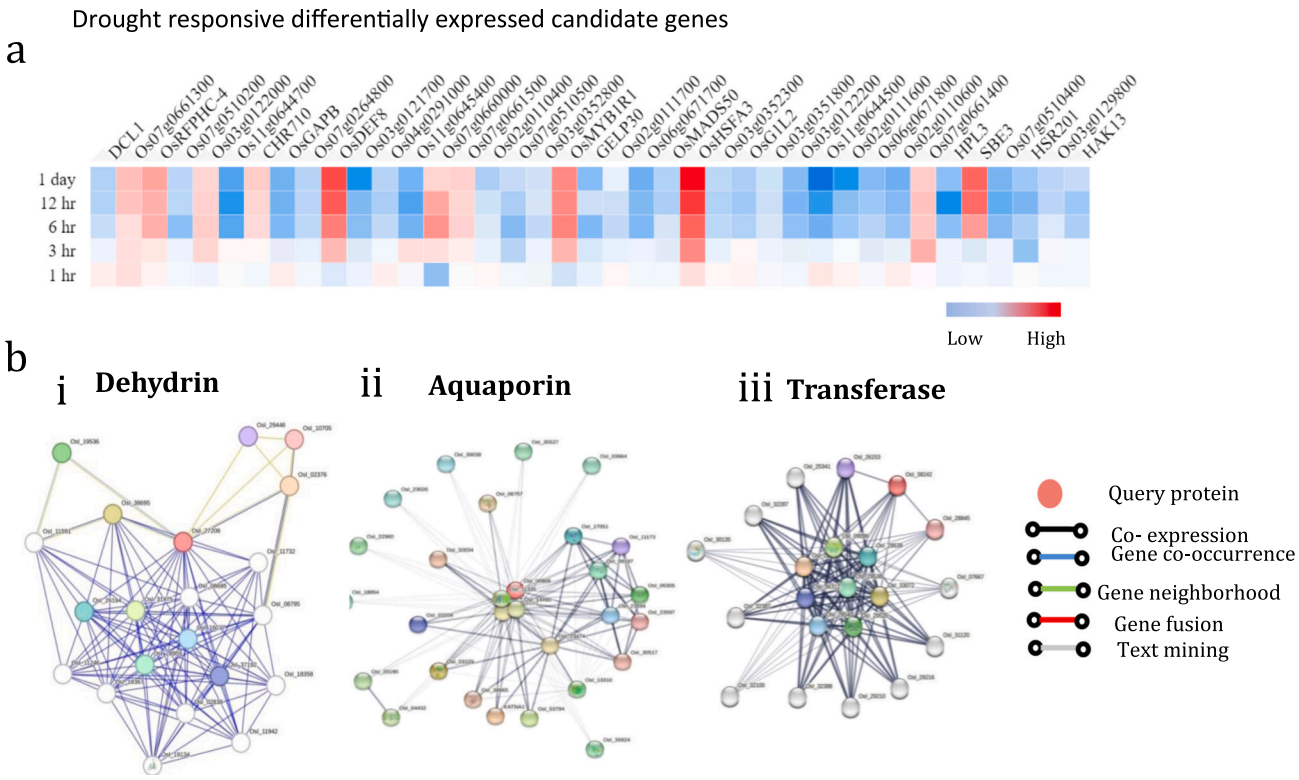

Fig. 10. (a) Differential expression of 44 candidate genes under drought as obtained from the NetRex database. (b) The core protein-protein interaction (PPI) network of (i) Osl_27206_early response to dehydrin, (ii) Osl_00806_aquaporin, and (iii) Osl_38242_ transferase constructed using the STRING database. The nodes represent proteins and the edges represent interactions between proteins in the network. Annotation of the genes are given in Supplementary Tables S13, S14, and S15.

affected leaves that are formed in the successive phylloochron, which was also suggested by Farooq et al., 2010 [27]. These arguments led us to hypothesize that the leaf structural resources saved by reducing leaf area under drought are reallocated to an increase in the thickness of subsequent leaves that are formed, most probably by increasing the mesophyll tissue layers in the ab-adaxial direction or by adding epidermal cuticular layers, but that was not investigated in this study. This SLA-mediated adaptive-re-shaping of rice leaves might change leaf cells and tissues allometrically [86] and most likely contribute to the maintenance of leaf water potential through increased xylem size, which was earlier identified as a key trait in rice drought tolerance [87]. Thicker leaves also reduce the amount of diffuse light that penetrates inside the leaf, thus protecting leaves from photodamage in the desiccated mesophyll cells [23,88]; this is supported by the identification of qDRI3.2 which includes several genes known to protect plant cells from oxidative damage during drought stress. It is also likely that root architectural and functional traits play a role in maintaining water uptake in the panel studied here as suggested by the variation in canopy temperatures, a trait often considered as a proxy of deep root growth under drought. The role of root traits in the drought response of these lines, and their interaction with individual leaf traits, remains to be defined particularly for drought tolerant lines identified from this study.

Regarding the effects of flowering time on drought tolerance in this panel, longer duration genotypes with higher biomass accumulation in leaves and stems did not translate to better grain yield under drought, which was primarily found to be limited by low HI (Table S5). Although previous investigation of the relationship between drought response and plant height [89] hypothesized that taller genotypes are affected more by drought than the shorter genotypes, our results pointed to more complex interactions among leaf functional and morphological traits in determining yield. In addition to the innate differences in flowering time, a drought-induced delay in flowering time has also previously been reported as an important indicator of the level of drought stress [90–92] with the most drought-sensitive plants never reaching flowering stage. A robust negative correlation in DRI with Δ_DTF was observed in 2019DS (Fig. 4b), reflecting how flowering delay under drought tends to be reduced in drought-tolerant genotypes. Based on this criteria, we functionally classified each early, medium, and late flowering group by its capacity to retain normal flowering time, or to moderately or severely delay their flowering time under MDS, giving a total of 9 categories: 1. early flowering genotypes that flowered early under drought, 2. early flowering genotypes that flowered in the medium duration, 3. early flowering genotypes that flowered late, 4. early flowering genotypes that never flowered, 5. medium flowering genotypes that flowered in the medium duration, 6. medium flowering genotypes that flowered late, 7. medium flowering genotypes that never flowered, 8. late flowering genotypes that flowered late, and 9. late flowering genotypes that never flowered. Categories 1, 5, and 8 were analysed together as those were the genotypes that could maintain their flowering time similar to that under WW conditions and were referred to as “flowered on time (FT)”. Categories 2, 3, and 6 were analysed together as those were considered as responsive genotypes which responded by delaying flowering time and were referred to as “flowering moderately delayed (FMD)” categories, and Categories 4, 7, and 9 were grouped together as the most sensitive genotypes and referred to as “flowering severely delayed (FSD)”. Whereas other traits behaved similarly under drought, the associations of ΔCi with ΔWUE, ΔA, Δg_s and ΔE varied in their strength among these different groups, suggesting the drought response of these traits to be dependent on stress severity and that they interact differently to achieve drought tolerance (Fig. 11). Likewise, the positive interactions of ΔCi, a parameter indicative of the CO_2 inside the leaf and the leaf stomatal opening, with ΔA were distinctly faded in 2019DS as the genotypes lost resistance to drought (Fig. 11 b iii). Even though the relation of DRI with WUE_i was consistent across categories, lack of any

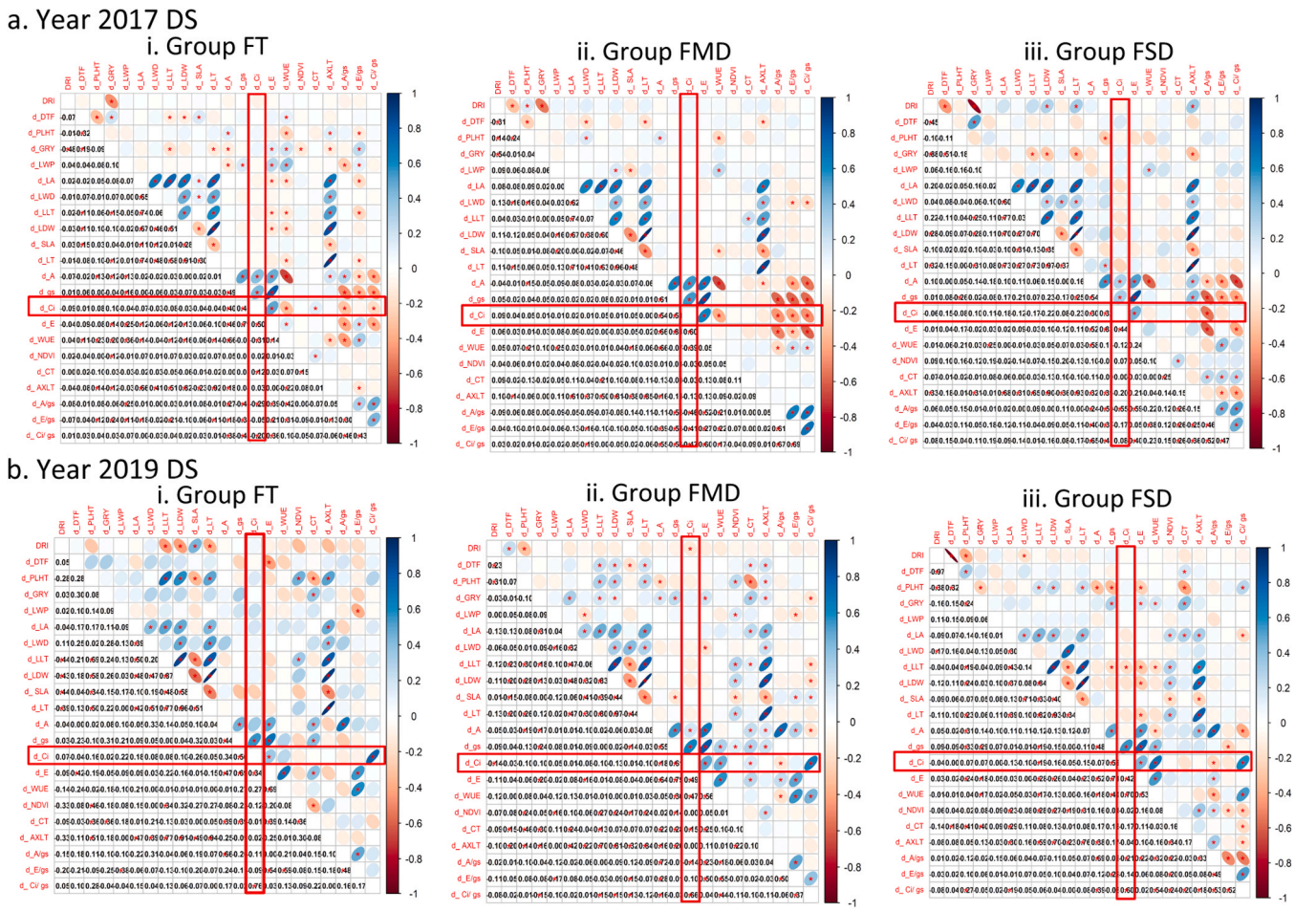

Fig. 11. Correlations of agro-morphological and functional characters of different functional groups (i) 1, 5, 8 (FT), (ii) 2,3,6 (FMD) and (iii) 4, 7, 9 (FSD) in (a) 2017DS and (b) 2019DS. The blue ellipses in the upper diagonal show positive interactions while the red ellipses show negative correlations among traits. The lower diagonal consists of the R^2 values. '*' designates significant ($P < 0.05$) correlations. The trait abbreviations are as in Table 1. For 2017DS; N = 368 for i, N = 188 for ii, and N = 66 entries for iii; in 2017DS, whereas N = 34 for i, N = 224 for ii, and N = 132 entries for iii. Red lines are to show the association ΔCi with other photosynthetic traits under moderate (a) and severe drought (b). Trait abbreviations are as in Table 1. FT: flowered on time, FMD; flowering modeately delayed, FSD: flowering severely delayed.

consistent relation of DRI directly with *E* suggested that reduction in transpiration was not the only strategy exhibited by these rice genotypes. Other mechanisms to achieve a higher WUE may include leaf developmental adjustments, as illustrated by the greater degree of leaf morphological adjustment with increasing DRI in the FT category (Fig. 12).

4.1. GWAS identified QTLs with drought responsive genes facilitating leaf hydraulics, photosynthesis, ROS maintenance, and leaf development in drought-stressed rice

The identified QTLs in our GWAS study possessed several genes known to play a vital role in drought tolerance as also confirmed by Rice-Pilaf gene network analysis which included genes from different biological processes commonly known to provide tolerance to drought stress (Fig. S8). Among the candidate genes related to DRI, aquaporins (in qDRI1.1) are well-known to be involved in drought tolerance in many model and crop species [93] such as grapevine [94], tomato [95], cotton [93,96], cereals [97] and others. In plants, five types of aquaporins are found: plasma membrane intrinsic proteins (PIPs), tonoplast intrinsic proteins (TIPs), NOD 26-like intrinsic proteins (NIPs), small basic intrinsic proteins (SIPs), and unclassified X intrinsic proteins (XIPs). In rice there are 33 aquaporin genes that play crucial roles in osmotic water fluxes during drought and recovery [98,99]. In our results, the candidate aquaporin gene at qDRI1.1 belonged to the MIP family and was found to function by interacting with other aquaporin genes, ATPase family genes, and glycerol 3 phosphate dehydrogenase, GAPDH (Fig. 10, Table S14) which interestingly turns to be a candidate gene in the locus qDRI3.1 (LOC_Os03g03720.1, Table2). As the function of GAPDH is crucial for maintaining cellular energy and carbon metabolism, interaction of GAPDH with aquaporins might play a vital role in sustaining photosynthesis under drought stress.

Another important candidate gene was the early response dehydrin in qDRI7.2, which has previously been reported to have a role in drought tolerance [100]. In plant cells, dehydrin genes are induced by dehydration stress, maintain cell stabilization, and maintain homeostasis by accumulation of hydrophilic dehydrin proteins [101]. Dehydrins contribute to withstanding drought stress by eliminating free radicals, protecting macromolecules, and binding metal ions [89]. The identified dehydrin in qDRI7.2 was found to be interacting with peroxidase and senescence domain containing proteins which suggests a possible function of qDRI7.2 in drought tolerance via better ROS scavenging. The overexpression of rice dehydrin gene OsDhn1 was found to increase drought and salinity tolerance in rice by scavenging of reactive oxygen species (ROS) [102].

In addition to aquaporin and dehydrin genes, DRI QTL qDRI2.1 included the 1,4-alpha-glucan-branching enzyme, HSF-type DNA binding domain containing protein, an RNA helicase, a SNF2 family protein,

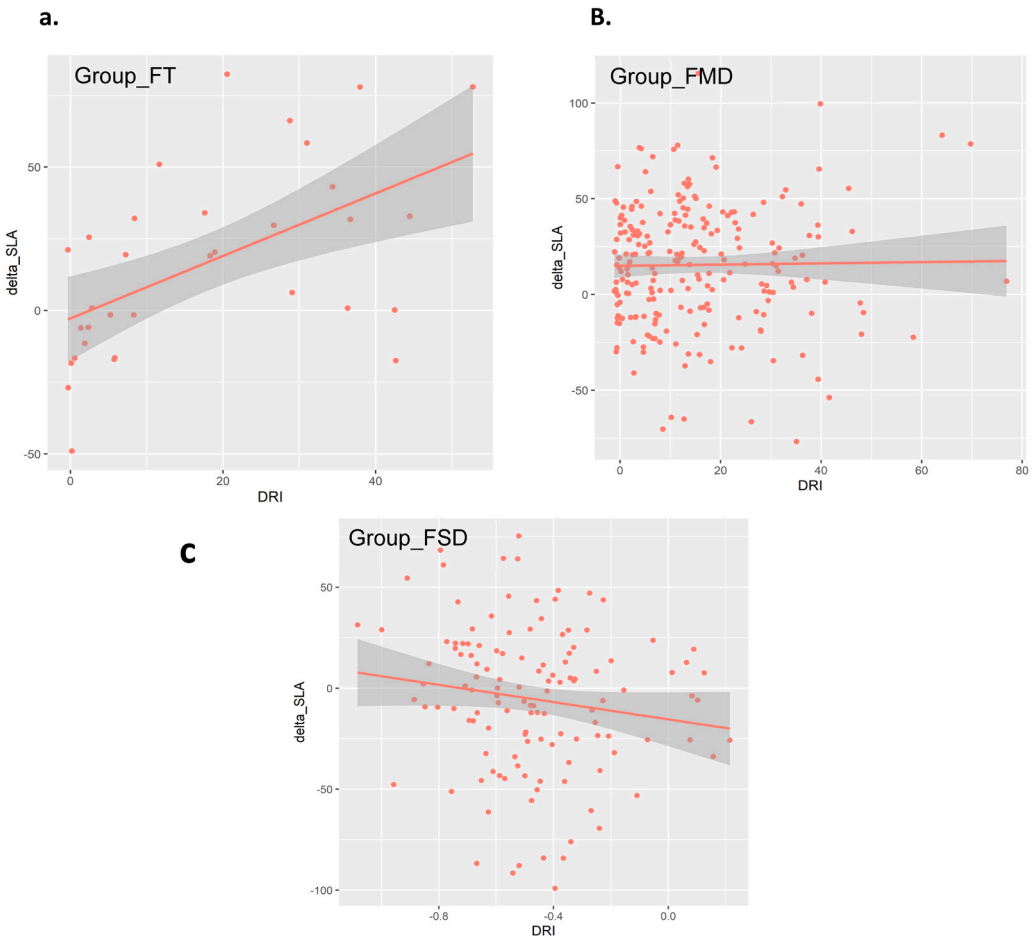

Fig. 12. Drought-induced leaf adjustment in SLA in different functional groups; FT (a), FMD (b) and FSD (c) in 2019 DS. FT: flowered on time, FMD; flowering modeately delayed, FSD: flowering severely delayed.

a WD repeat containing protein, and a WAK receptor like protein kinase genes (qDRI2.2), all of which may be considered relevant to drought tolerance. The 1,4-alpha-glucan-branching enzyme may provide required energy from metabolizing starch during drought stress. It has been reported that plants lacking 1,4-alpha-glucan-branching enzyme are more sensitive to drought [103]. Sucrose non-fermenting 2 or the SNF2 proteins are known to get differentially expressed under stress and contribute to drought tolerance through activating dehydration responsive genes and ABA signaling (104) Candidate gene HSF, the plant heat shock factor protein, has been reported to enhance the heat and drought tolerance of rice by triggering transcription factors such as *ZIP*, *NAC*, *WRKY,* and eventually activating the HSP proteins [105]. WD repeat containing proteins also play a role in stress tolerance [106] by acting as transition proteins which help in integrating secondary structures of stress tolerant proteins [107]. OsWAK11 - OsWAK receptor-like protein kinase, negatively regulates salt stress responses by Inhibiting ethylene production [108]. The role of calcium/calmodulin dependent protein kinases is well known as an important signal molecule to transfer stress signals and provide tolerance to salt and drought by preventing membrane lipid peroxidation [109,110]. Similarly, flavonoids are known to provide protection to photodamage and thus tolerance to drought in species like *Reaumuria soongorica* [111]. These candidate gene functions add confidence to understand the major role of our identified DRI QTLs in drought tolerance, which can be considered for integration in drought breeding programs for yield improvement.

Association of HI with drought tolerance can be the result of better mobilization of carbohydrates to reproductive organs [112]. In the GWAS result of HI under drought, we have found a single locus with two similar genes of the transferase family protein. Interestingly, these transferase proteins interact with AAI domain (Alpha-Amylase Inhibitors) containing proteins which potentially increase yield and drought tolerance in rice [113].

The genes for actin-depolymerizing factors reported in qSLA7.1 function in developing actin filaments which determine cell size and shape might be involved in controlling leaf size under drought as increased cell division and expansion may be needed to change leaf thickness under drought. The association of the known drought-induced genes, such as the short chain dehydrogenase/reductase protein [114], SNF2 family N-terminal domain containing protein [104] in qSLA4.1 and qSLA3.1 regions suggested that drought-induced leaf developmental adjustments influence functioning of these known drought tolerance genes.

None of the marker-trait associations could cross the –logP= 5 threshold for WUE under drought, which suggested the complex nature of this trait. However, the QTLs selected at a suggestive threshold of -logP= 4.5 showed co-occurrence of IQ calmodulin-binding motif domain containing protein, expressed (LOC_Os01g09790.1); transporter family protein, putative, expressed (LOC_Os11g42430.1) which have known functions in drought tolerance (Table3) and influenced water use efficiency [115] by inducing calcium mediated signaling under drought. The presence of Myb transcription factors and F box proteins in qWUE1.1 suggested a possible role of these genes in leaf architecture under drought to regulate water use efficiently [116]. It was also interesting to note that many of these identified genes were reportedly expressed in pre- and post- emergence inflorescences (Table S11), which pointed towards possible effects of the identified QTLs on maintaining

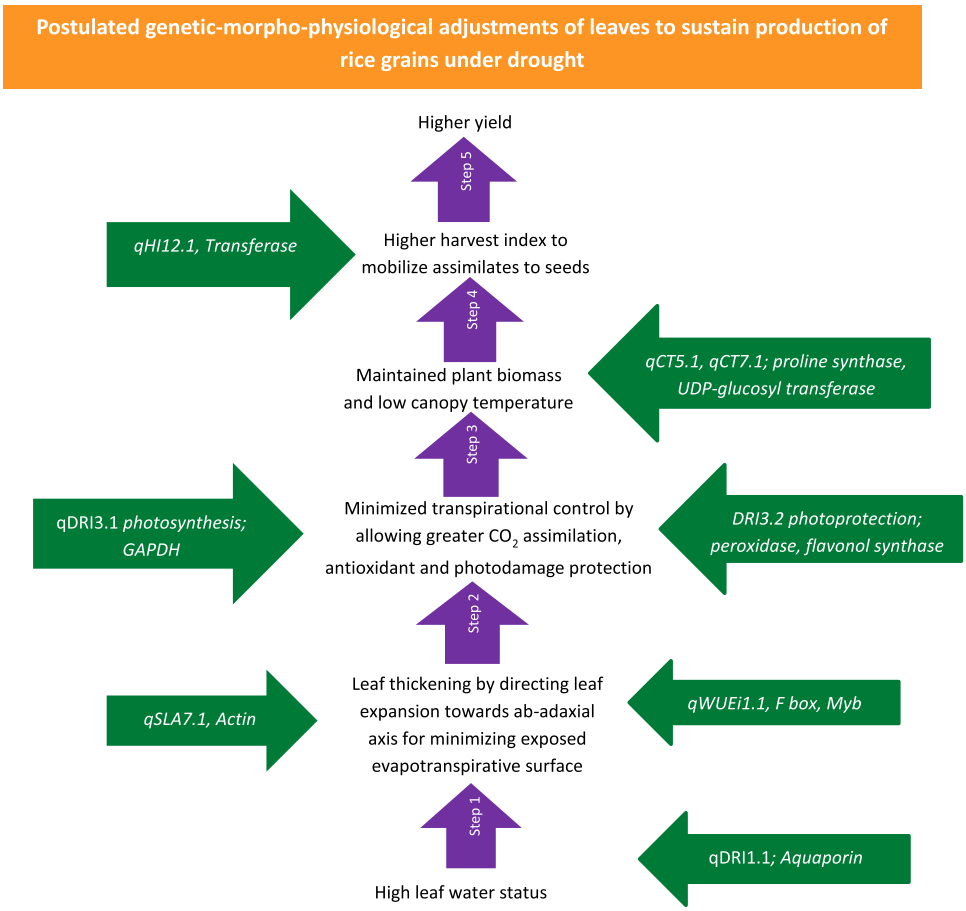

Fig. 13. A predicted framework along with genotypic interactions showing a conceptualization of achieving greater rice crop yield under drought. The central function of the identified QTLs and major candidate genes associated with the function are mentioned in *italics* in the flowchart. Details of the genes are in Table 2 and Table 3.

viability of reproductive organs to produce seeds under drought. Finally, it is interesting to observe GWAS peaks at a similar region as the drone-acquired CT data and manually estimated DRI. The main gene present in both the QTLs, UDP-glucosyltransferase, is known for regulating grain size and abiotic stress tolerance associated with metabolic flux redirection in rice [117]. Another gene present in qCT5.1, proline synthase (LOC_Os05g05740.1), also might be a good candidate gene to test for drought tolerance as it is known for maintaining osmolyte – water balance during drought [105 [118].

4.2. *Conceptualization of the integration of leaf traits, photosynthesis, and candidate genes contributing to yield under drought*

Fig. 13 depicts an overall conceptualization based on our results, suggesting how leaf morphology, function, and genetics interact for grain yield under drought. The comparison between the initial, drought-adapted, and final correlations of traits to DRI over two seasons (Fig. S9) showed that some of the traits retain higher values to maintain a higher DRI, whereas some traits maintain lower values with increasing DRI. The traits which consistently increased with increasing yield under drought were ψ_{Leaf}, PLHT, GRY, BM, HI, and all of the leaf morphological traits including LA, LWD, LLT, LDW, LT, and the photosynthetic traits *A*, g_s, and even *E*. On the other hand, the values of some traits remained consistently low under drought (NDVI, DTF, Ci/g_s) and some traits responded seasonally according to drought severity (SLA, WUE_i, CT, A×LT, A/g_s, E/g_s). This led us to predict a plausible model for rice drought tolerance wherein maintaining higher leaf water levels supports higher photosynthetic rates followed by functional utilization of assimilated carbon for increased final grain yield. While water conservation can be achieved under drought both by thickening the leaves or by rolling the leaves, the former can minimize water loss by minimizing the evaporative surface of the leaves; the correlations of SLA adjustment with DRI observed here indicated that thickening conferred greater benefits to productivity. This may be due to the continuation of photosynthesis under drought in thicker leaves that does not occur to the same extent in rolled leaves. Therefore, broader leaves combined with better plasticity of redistributing leaf tissues along the ab-adaxial axis in subsequent leaves formed in the phyllochron during water deficit conditions may therefore be considered a drought-resilient trait. This may also explain the inconsistency among studies that consider simple relationships between single leaf traits with drought. Leaf reshaping to increase thickness may contribute more to drought tolerance than mere unidirectional changes in leaf length or in leaf width, helping to sustain photosynthesis rates by maintaining leaf *Ci* under drought.

Overall, our results indicate that although water saving by reducing stomatal conductance in rice is a common drought response, it does not always provide tolerance or capacity to produce high grain yield under drought. In contrast to the observations of drought tolerance being conferred by transpirational control of water loss in many dryland crops [75,119], our results suggest that drought tolerant lowland rice exhibits more of a strategy of “aggressive water use”, the term as mentioned by [93], to produce more grain under drought conditions. This approach has recently been also established in some tree species [21,120,121]. The identification of DRI QTLs and candidate genes including aquaporin, dehydrin, and genes related to antioxidant scavenging which play major roles in cellular transport, water retention, and osmolyte balance,

association of actin for probable leaf cell division controlling size and shape further supports our concept. Finally, we also identified nine genotypes (Table S16) that consistently exhibited high DRI values in both seasons. Although no specific trait could be consistently linked to DRI in these genotypes across both seasons, suggesting genotype specific drought response strategies, leaf adjustments under drought were notable in terms of reduced leaf length and SLA, and increased leaf thickness. All of these genotypes showed drought-induced leaf thickening, with eight of them showing an increase in leaf length, pointing to a benefit of leaf adaptive adjustments under drought. In contrast, we could not find any leaf thickness increment in the check variety NSIC Rc222 which is drought susceptible. Interestingly, NSIC Rc222 showed one of the lowest canopy temperatures (Fig. 1b), and there was a large range of CT at the start of the drought stress treatment across the selected varieties indicating that many different traits and mechanisms could result in drought tolerance at the yield level.

5. Conclusions

Our study has attempted to identify the main foliar phenotypic traits that can provide drought resilience to rice. The results suggested an important role of leaf reshaping in maintaining high ψ_{Leaf} and higher photosynthetic performance under drought which may lead to higher grain yields in rice under drought conditions. The genetics underlying the production of high grain yield under drought indicated genes involved in water transport, antioxidant protection, photosynthesis and leaf development in the identified QTL regions, as well as co-localization of qDRI7.1 and qDRI7.1 suggesting a crucial role of leaf pigment mediated photoprotection, maintaining ψ_{Leaf} and transpiration for cooler canopy temperature contributing to the production of higher grain under drought. Overall, our results highlight the importance of phenotypic traits that facilitate maintenance of high transpiration rates even in depleting soil moisture specifically for rice. An overall framework was presented, with roles of candidate genes in each step of the progression towards a better harvest under drought. Finally, we have identified the best-performing donors that can be considered in drought breeding for improving grain yield under drought by leaf trait adjustments.

Author contributions

Author WPQ, AH, and KLM conceptualized the field drought study; JC, MJD, MRL, MR-Q, MDO analysed phenotypic data; PMM, MEBN, MN conducted the experiment in WW and drought fields; SK collected, processed, and analysed drone data; MDO and DC conducted GWAS; JC, AH, SC, WPQ, KLM, and all authors contributed to constructing the paper.

Funding

This research is supported by the CGIAR Research Program "Global Rice Science Partnership (GRISP)".

Declaration of Competing Interest

The authors declare that they have no known competing financial interests or personal relationships that could have appeared to influence the work reported in this paper.

Acknowledgements

We thank the Molecular Genetics team of the T.T. Chang Genetic Resources Center for the field management and phenotyping of agro-morphological traits. We are thankful to IRRI's field and laboratory technicians of the IRRI C4 Rice team and IRRI Stress Physiology teams for helping assisting in laboratory and field work and field management. We acknowledge the IRRI Genetic Resource team for providing us the seed material for this study. We especially thank Irma Canicosa for her contribution to gas-exchange measurements in the field.

Appendix A. Supporting information

Supplementary data associated with this article can be found in the online version at doi:10.1016/j.cpb.2026.100660.

Data availability

Data generated and analyzed during the current study will be uploaded to the IRRI Dataverse site upon publication.

References

[1] M.A. Hassan, N. Dahu, T. Hongning, Z. Qian, Y. Yueming, L. Yiru, W. Shimei, Drought stress in rice: morphophysiological and molecular responses and marker-assisted breeding, Front. Plant. Sci. 14 (2023) 1215371, https://doi.org/10.3389/fpls.2023.121537.

[2] A. Wahab, G. Abdi, M.H. Saleem, B. Ali, S. Ullah, W. Shah, S. Mumtaz, G. Yasin, M. Crina, R. Marc, Plants' physio-biochemical and phyto-hormonal responses to alleviate the adverse effects of drought stress: a comprehensive review, Plants 11 (2022) 1620, https://doi.org/10.3390/plants11131620.

[3] X. Wang, J. Huang, S. Peng, D. Xiong, Leaf rolling precedes stomatal closure in rice (*Oryza sativa*) under drought conditions, J. Exp. Bot. 74 (21) (2023) 6650–6661, https://doi.org/10.1093/jxb/erad316. PMID: 37551729.

[4] B. Jongdee, S. Fukai, M. Cooper, Leaf water potential and osmotic adjustment as physiological traits to improve drought tolerance in rice, Field Crops Res. 76 (2–3) (2002) 153–163.

[5] D. Panda, S.S. Mishra, P.K. Behera, Drought tolerance in rice: focus on recent mechanisms and approaches, Rice Sci. 28 (2) (2021) 119–132, https://doi.org/10.1016/J.RSCI.2021.01.002.

[6] M. Qi, X. Liu, Y. Li, H. Song, Z. Yin, F. Zhang, Q. He, Z. Xu, G. Zhou, Photosynthetic resistance and resilience under drought, flooding and rewatering in maize plants, Photosynth. Res. 148 (1-2) (2021) 1–15, https://doi.org/10.1007/s11120-021-00825-3. Epub 2021 Mar 4. PMID: 33661466.

[7] Y.A.N. Reddy, Y.N.Priya Reddy, V. Ramya, L.S. Suma, A.B.Narayana Reddy, S. Sanjeev Krishna, Drought adaptation: Approaches for crop improvement, Editor (s): Mohar Singh, Salej Sood, In Woodhead Publishing Series in Food Science, Technology and Nutrition, Chapter 8. Millets and Pseudo Cereals, Woodhead Publishing, 2021, pp. 143–158. Chapter 8.

[8] H. Nayyar, D. Gupta, Differential sensitivity of C3 and C4 plants to water deficit stress: association with oxidative stress and antioxidants, Environ. Exp. Bot. 58 (2006) 106–113, https://doi.org/10.1016/j.envexpbot.2005.06.021.

[9] D. Wach, P. Skowron, An overview of plant responses to the drought stress at morphological, physiological and biochemical levels, Pol. J. Agron. 50 (2022) 25–34.

[10] H.C. Lin, J. Dionora, D. Chebotarov, Ma.R. Laza, Ma.E.B. Naredo, P.A. Muyco, S. Klassen, A. Henry, W.P. Quick, K. McNally, Phenotyping of the 3K indica rice panel for physiological and morphological traits, Current Plant Biology 47 (2026) 100613, https://doi.org/10.1016/j.cpb.2026.100613.

[11] Ü. Niinemets, Variation in leaf photosynthetic capacity within plant canopies: optimization, structural, and physiological constraints and inefficiencies, Photosynth. Res. 158 (2023) 131–149, https://doi.org/10.1007/s11120-023-01043-9.

[12] W. Ouyang, P.C. Struik, X. Yin, J. Yang, Stomatal conductance, mesophyll conductance, and transpiration efficiency in relation to leaf anatomy in rice and wheat genotypes under drought, J. Exp. Bot. 68 (18) (2017) 5191–5205, https://doi.org/10.1093/jxb/erx314.

[13] A.J. Cal, M. Sanciangco, M.C. Rebolledo, D. Luquet, R.O. Torres, K.L. McNally, A. Henry, Leaf morphology, rather than plant water status, underlies genetic variation of rice leaf rolling under drought, Plant Cell Environ. 42 (5) (2019) 1532–1544, https://doi.org/10.1111/pce.13514. Epub 2019 Feb 20. PMID: 30620079; PMCID: PMC6487826.

[14] M.D. Mahalle, S.K. Chetia, P.C. Dey, et al., Assessing the leaf shape dynamic through marker–trait association under drought stress in a rice germplasm panel, Plant Genet. Resour. Charact. Util. 19 (6) (2021) 477–483, https://doi.org/10.1017/S1479262121000587.

[15] W. Yu, S.J. Burgess, E.Md Becker, S.P. Long, Photosynthesis in the fleeting shadows: an overlooked opportunity for increasing crop productivity? Plant J. 101 (4) (2020) 874–884, https://doi.org/10.1111/tpj.14663.

[16] A.J. Burgess, C. Masclaux-Daubresse, G. Strittmatter, A.P.M. Weber, S.H. Taylor, J. Harbinson, et al., Improving crop yield potential: underlying biological processes and future prospects (Available from:), Food Energy Secur. 12 (2023) e435, https://doi.org/10.1002/fes3.435.

[17] A. Henry, V.R.P. Gowda, O. Torres, K.L. Rolando, R. McNally, Serraj, Variation in root system architecture and drought response in rice (*Oryza sativa*): Phenotyping of the OryzaSNP panel in rainfed lowland fields, Field Crops Res. 120 (2011) 205–214.

[18] Q. Liao, D. Chebotarov, M.S. Islam, M.R. Quintana, M.A. Natividad, M. De Ocampo, J.C. Beredo, R.O. Torres, Z. Zhang, H. Song, A.H. Price, K.L. McNally, Amelia Henry, Aus rice root architecture variation contributing to grain yield under drought suggests a key role of nodal root diameter class, Plant Cell Environ 45 (2022) 854–870, https://doi.org/10.1111/pce.14272.

[19] J.L. Siangliw, B. Thunnom, M.A. Natividad, M.R. Quintana, D. Chebotarov, K. L. McNally, J.P. Lynch, K.M. Brown, A. Henry, Response of Southeast Asian rice root architecture and anatomy phenotypes to drought stress, Front. Plant. Sci. 19 (2022).

[20] H. Bochmann, M. Klein, A. Henry, H. Faßbender, M. De Ocampo, J. Kant, M. Watt, Rice cycles between drought and well-watered-adapted phenotypes by changing lateral root formation, Ann. Bot. 136 (5-6) (2025) 1265–1277, https://doi.org/10.1093/aob/mcaf173.

[21] I.J. Wright, N. Dong, V. Maire, I.C. Prentice, M. Westoby, S. Díaz, R.V. Gallagher, et al., Global climatic drivers of leaf size, Science 357 (6354) (2017) 917–921.

[22] J. Chatterjee, J. Dionora, A. Elmido-Mabilangan, S. Wanchana, V. Thakur, A. Bandyopadhyay, et al., The Evolutionary Basis of Naturally Diverse Rice Leaves Anatomy, PLoS. ONE 11 (10) (2016) e0164532, https://doi.org/10.1371/journal.pone.0164532.

[23] M. Momayyezi, A.M. Borsuk, C.R. Brodersen, M.E. Gilbert, G. Théroux-Rancourt, D.A. Kluepfel, A.J. McElrone, Desiccation of the leaf mesophyll and its implications for CO_2 diffusion and light processing, Plant Cell Environ. 45 (5) (2022) 1362–1381, https://doi.org/10.1111/pce.14287.

[24] M.G. Tjoelker, E.J. Veneklaas, R. Villar, The worldwide leaf economics spectrum, Nature 428 (2004) 821–827.

[25] C.-G. Liu, X.-Q. Zhou, D.-G. Chen, L.-J. Li, J.-C. Li, Y.-D. Chen, Natural variation of leaf thickness and Its association to yield traits in indica rice, J. Integr. Agric. 13 (2) (2014) 316–325.

[26] N. Hamaoka, H. Yasui, Y. Yamagata, et al., A hairy-leaf gene, BLANKET LEAF, of wild *Oryza nivara* increases photosynthetic water use efficiency in rice, Rice 10 (20) (2017), https://doi.org/10.1186/s12284-017-0158-1.

[27] M. Farooq, N. Kobayashia, O. Itoc, A. Wahidd, R. Serraj, Broader leaves result in better performance of indica rice under drought stress, J. Plant Physiol. 167 (2010) 1066–1075.

[28] A. Khan, F. Shen, L. Yang, W. Xing, B. Clothier, Limited Acclimation in Leaf Morphology and Anatomy to Experimental Drought in Temperate Forest Species, Biology 11 (2022) 1186, https://doi.org/10.3390/biology11081186.

[29] T. Liu, S. Li, H. Du, J. Cui, S. Xu, J. Wang, H. Liu, D. Zou, W. Lu, H. Zheng, The Identification of Drought Tolerance Candidate Genes in *Oryza sativa* L. ssp. Japonica Seedlings through Genome-Wide Association Study and Linkage Mapping, Agriculture 14 (2024) 603, https://doi.org/10.3390/agriculture14040603.

[30] K.L. Adjah, M.D. Asante, M. Frei, A. Toure, M. Aziadekey, L. Wu, A. Wairich, D. Dzorkpe Gamenyah, S. Yadav, Leaf reflectance and physiological attributes monitoring differentiate rice cultivars under drought-stress and non-stress conditions, Cogent Food & Agric. 11 (1) (2025) 2453086, https://doi.org/10.1080/23311932.2025.2453086.

[31] H.S. Jasmine, K.U. Ahamed, J.K. Biswas, Study on the Leaf Traits of Aus Rice Varieties in Various Soil Moisture Levels, Open. Access. Libr. J. 10 (2023) e9254.

[32] A.K. Biswal, A. Kohli, Cereal flag leaf adaptations for grain yield under drought: knowledge status and gaps, Mol. Breed. 31 (2013) 749–766, https://doi.org/10.1007/s11032-013-9847-7.

[33] U. Bhandari, A. Gajurel, B. Khadka, I. Thapa, I. Chand, D. Bhatta, A. Poudel, M. Pandey, S. Shrestha, J. Shrestha, Morpho-physiological and biochemical response of rice (*Oryza sativa* L.) to drought stress: A review, ISSN 2405-8440, Heliyon 9 (3) (2023) e13744, https://doi.org/10.1016/j.heliyon.2023.e13744.

[34] F.A. Pradhan, J. Zhang, T.P.P. Sharma, L. Nanzad, D. Zhang, A.M. Seka, N. Ahmed, S.S. Hasan, M.Z. Hoque, H.P. Mohana, Projection of future drought and its impact on simulated crop yield over South Asia using ensemble machine learning approach, Sci. Total. Environ. 807 (3) (2022) 151029.

[35] S. Pandey, H. Bhandari, Drought: Economic Costs and Research Implications, in: R. Serraj, J. Bennett, B. Hardy (Eds.), Drought Frontiers in Rice: Crop Improvement for Increased Rainfed Production, World Scientific Publishing, Singapore, 2008, pp. 3–17.

[36] M.H. Dar, et al., Drought tolerant rice for ensuring food security in eastern India, Sustainability 12 (6) (2020) 2214, https://doi.org/10.3390/su12062214.

[37] S. Perween, A. Kumar, F. Adan, J. Kumar, P. Raj, A. Kumar, Correlation and path analysis of yield components in rice (Oryza sativa L.) under irrigated and reproductive stage drought stress condition, Current Journal Applied Science Technology 39 (8 (2020) 60–68, https://doi.org/10.9734/cjast/2020/v39i830593.

[38] W. Wang, R. Mauleon, Z. Hu, et al., Genomic variation in 3,010 diverse accessions of Asian cultivated rice, Nature 557 (2018) 43–49, https://doi.org/10.1038/s41586-018-0063-9.

[39] The 3,000 rice genomes project, The 3,000 rice genomes project, GigaSci 3 (7) (2014), https://doi.org/10.1186/2047-217X-3-7.

[40] H.C. Lin, J. Dionora, D. Chebotarov, M.R. Laza, Ma.E.B. Naredo, P.A. Muyco, S. Klassen, A. Henry, W.P. Quick, K.L. McNally, Diversity of photosynthesis-related and high-throughput phenotyping traits in indica rice, Curr. Plant. Biol. 47 (2026) 100613, https://doi.org/10.1016/j.cpb.2026.100613.

[41] F.R. Bidinger, V. Mahalakshmi, G.D.P. Rao, Assessment of drought resistance in pearl millet (*Pennisetum americanum* (L.) Leeke). II. Estimation of genotype response to stress, Aust. J. Agric. Res. 38 (1987) 49–59.

[42] L. Mansueto, R.R. Fuentes, F.N. Borja, J. Detras, J.M. Abriol-Santos, D. Chebotarov, M. Sanciangco, K. Palis, D. Copetti, A. Poliakov, I. Dubchak, V. Solovyev, R.A. Wing, R.S. Hamilton, R. Mauleon, K.L. McNally, N. Alexandrov, Rice SNP-seek database update: new SNPs, indels, and queries, Nucleic Acids Res. 45 (2016) D1075–D1081.

[43] L. Mansueto, R.R. Fuentes, D. Chebotarov, F.N. Borja, J. Detras, J.M. Abriol-Santos, K. Palis, A. Poliakov, I. Dubchak, V. Solovyev, R.S. Hamilton, K. L. McNally, N. Alexandrov, R. Mauleon, SNP-Seek II: a resource for allele mining and analysis of big genomic data in *Oryza sativa*, Curr. Plant. Biol. 78 (2016) 16–25.

[44] J. C. O'Toole, R. T. Cruz, Leaf rolling and transpiration, Plant. Sci. Lett. 16 (1) (1979) 111–114, https://doi.org/10.1016/0304-4211(79)90015-4.

[45] Y. Lu, Z. Hao, C. Xie, J. Crossa, J.-L. Araus, S. Gao, Y. Xu, Large-scale screening for maize drought resistance using multiple. selection criteria evaluated under water-stressed and well-watered. environments, Field Crops Res. 124 (2011) 37–45, https://doi.org/10.1016/j.fcr.2011.06.003.

[46] D. Bates, M. Mächler, B. Bolker, S. Walker, Fitting Linear Mixed-Effects Models Using *lme4*, J. Stat. Softw. 67 (2015) 1–48, https://doi.org/10.18637/JSS.V067.I01.

[47] L. Mansueto, R.R. Fuentes, D. Chebotarov, N.F. Borja, J. Detras, J.M. Abriol-Santos, K. Palis, A. Poliakov, I. Dubchak, V. Solovyev, R.S. Hamilton, K. L. McNally, N. Alexandrov, R. Mauleon, SNP-Seek II: A resource for allele mining and analysis of big genomic data in Oryza sativa, Curr. Plant Biol. 7 (8) (2016) 16–25.

[48] C.C. Chang, C.C. Chow, L.C. Tellier, S. Vattikuti, S.M. Purcell, J.J. Lee, Second-generation PLINK: rising to the challenge of larger and richer datasets, GigaScience 4 s13742–015–0047–8 (2015). https://doi.org/10.1186/s13742-015-0047-8.

[49] P.J. Bradbury, Z. Zhang, D.E. Kroon, T.M. Casstevens, Y. Ramdoss, E.S. Buckler, TASSEL: software for association mapping of complex traits in diverse samples, Bioinformatics 23 (2007) 2633–2635, https://doi.org/10.1093/bioinformatics/btm308).

[50] Z. Zhang, et al., Mixed linear model approach adapted for genome-wide association studies, Nat. Genet. 42 (2010) 355–360.

[51] A.E. Lipka, F. Tian, Q. Wang, J. Peiffer, M. Li, P.J. Bradbury, M.A. Gore, E. S. Buckler, Z. Zhang, GAPIT: genome association and prediction integrated tool, Bioinformatics 28 (2012) 2397–2399.

[52] R.M. West, Best practice in statistics: The use of log transformation, Ann. Clin. Biochem. 59 (3) (2022) 162–165, https://doi.org/10.1177/00045632211050531. Epub 2021 Oct 19. PMID: 34666549; PMCID: PMC9036143.

[53] Li, L. Ji, Adjusting multiple testing in multilocus analyses using the eigenvalues of a correlation matrix, Heredity 95 (2005) 221–227, https://doi.org/10.1038/sj.hdy.6800717.

[54] J. Yuan, X. Wang, Y. Zhao, et al., Genetic basis and identification of candidate genes for salt tolerance in rice by GWAS, Sci. Rep. 10 (2020) 9958, https://doi.org/10.1038/s41598-020-66604-7.

[55] A.M.S. Shrestha, M.E.M. Gonzales, P.C.L. Ong, P. Larmande, H.S. Lee, J.U. Jeung, A. Kohli, D. Chebotarov, R.P. Mauleon, J.S. Lee, K.L. McNally, RicePilaf: a post-GWAS/QTL dashboard to integrate pangenomic, coexpression, regulatory, epigenomic, ontology, pathway, and text-mining information to provide functional insights into rice QTLs and GWAS loci, Gigascience Jan. 2 13 (2024) giae013, https://doi.org/10.1093/gigascience/giae013. PMID: 38832465; PMCID: PMC11148593.

[56] D. Szklarczyk, A.L. Gable, D. Lyon, A. Junge, S. Wyder, J. Huerta-Cepas, M. Simonovic, N.T. Doncheva, J.H. Morris, P. Bork, L.J. Jensen, C.V. Mering, STRING v11: protein-protein association networks with increased coverage, supporting functional discovery in genome-wide experimental datasets, Jan 8, Nucleic Acids Res. 47 (D1) (2019) D607–D613, https://doi.org/10.1093/nar/gky1131.

[57] S. Sircar, M. Musaddi, N. Parekh, NetREx: Network-based Rice Expression Analysis Server for abiotic stress conditions, August 6, Database (2022) baac060.

[58] J. Xiong, H. Wang, Z. Zhong, S. Li, P. Qin, Emerging strategies to improve heat stress tolerance in crops, aBIOTECH 6 (1) (2025) 97–115, https://doi.org/10.1007/s42994-024-00195-z. PMID: 40060179; PMCID: PMC11889333.

[59] Y.C.F. Salsinha, D. Maryani, Y.A. Indradewa Purwestri, D. Rachmawati, Leaf physiological and anatomical characters contribute to drought tolerance of Nusa Tenggara Timur local rice cultivars, J. Crop. Sci. Biotechnol. 24 (2021) 337–348.

[60] J.M. Lilley, S. Fukai, Effect of timing and severity of water-deficit on 4 diverse rice cultivars.2. Physiological-responses to soil-water deficit, Field Crops Res. 37 (1994) 215–223.

[61] A. Latif, S. Ying, P. Cuixia, N. Ali, Rice Curled Its Leaves Either Adaxially or Abaxially to Combat Drought Stress, Rice Sci. 30 (5) (2023) 405–416.

[62] P. Mangena, Water stress: Morphological and anatomical changes in soybean (*Glycine max* L.) plants, Andjelkovic V. Plant. Abiotic Stress and Responses to Climate Change, Intech Open, 2018, pp. 9–31.

[63] B. Parent, B. Suard, R. Serraj, F. Tardieu, Rice leaf growth and water potential are resilient to evaporative demand and soil water deficit once the effects of root system are neutralized, Plant Cell Environ. 33 (8) (2010) 1256–1267, https://doi.org/10.1111/j.1365-3040.2010.02145.x. Epub 2010 Mar 18. PMID: 20302604.

[64] I. Yavas, M.A. Jamal, K.U. Din, S. Ali, S. Hussain, M. Farooq, Drought-Induced Changes in Leaf Morphology and Anatomy: Overview, Implications and Perspectives, Pol. J. Environ. Stud. 33 (2) (2024) 1517–1530, https://doi.org/10.15244/pjoes/174476.

[65] L.-L. Liu, Y.Q. Deng, X.X. Dong, C.F. Wang, F. Yuan, G.L.- Han, B.S. Wang, ALDH2C4 regulates cuticle thickness and reduces water loss to promote drought tolerance, ISSN 0168-9452, Plant. Sci. 323 (2022) 111405, https://doi.org/10.1016/j.plantsci.2022.111405.

[66] S. Kumar S, S.P. Singh Tripathi, A. Prasad, F. Akter, Md.A. Syed, J. Badri, S.P. Das, R. Bhattarai, M.A. Natividad, M. Quintana, C. Venkateshwarlu, A. Raman, S. Yadav, S.K. Singh, P. Swain, A. Anandan, R.B. Yadaw, N.P. Mandal, S. B. Verulkar, A. Kumar, A. Henry, Rice breeding for yield under drought has selected for longer flag leaves and lower stomatal density, J. Exp. Bot. 72 (13) (2021) 4981–4992, https://doi.org/10.1093/jxb/erab160.

[67] A. Fathi, D.B. Tari, Effect of drought stress and its mechanism in plants, Int. J. Life Sci. 10 (1) (2016) 1–6.

[68] A. Raman, S. Verulkar, N. Mandal, et al., Drought yield index to select high yielding rice lines under different drought stress severities, Rice 5 (2012) 31, https://doi.org/10.1186/1939-8433-5-31.

[69] S. Dixit, A. Singh, A. Kumar, Rice Breeding for High Grain Yield under Drought: A Strategic Solution to a Complex Problem, Int. J. Agron. (2014), https://doi.org/10.1155/2014/863683.

[70] H. Upadhyaya, S.K. Panda, Chapter 9 - Drought Stress Responses and Its Management in Rice, Editor(s): Mirza Hasanuzzaman, Masayuki Fujita, Kamrun Nahar, Jiban Krishna Biswas. Advances in Rice Research for Abiotic Stress Tolerance, Woodhead Publishing, 2019, pp. 177–200.

[71] A. Gupta, A. Rico-Medina, A.I. Caño-Delgado, The physiology of plant responses to drought, Science 368 (2020) 266–269, https://doi.org/10.1126/SCIENCE.AAZ7614.

[72] G. Melandri, H. AbdElgawad, D. Riewe, J.A. Hageman, H. Asard, G.T.S. Beemster, N. Kadam, K. Jagadish, T. Altmann, C. Ruyter- Spira, H. Bouwmeester, Biomarkers for grain yield stability in rice under drought stress, J. Exp. Bot. 71 (2) (2020) 669–683.

[73] Y. Yang, J. Yu, Q. Qian, et al., Enhancement of Heat and Drought Stress Tolerance in Rice by Genetic Manipulation: A Systematic Review, Rice 15 (2022) 67, https://doi.org/10.1186/s12284-022-00614-z.

[74] V. Vadez, J. Kholova, S. Medina, A. Kakkera, H. Anderberg, Transpiration efficiency: new insights into an old story, J. Exp. Bot. 65 (2014) 6141–6153, https://doi.org/10.1093/jxb/eru040.

[75] A. Henry, H. Stuart-Williams, S. Dixit, A. Kumar, Graham Farquhar, Stomatal conductance responses to evaporative demand conferred by rice drought-yield quantitative trait locus *qDTY12.1*, Funct. Plant. Biol. 46 (2019) 660–669.

[76] H.G. Jones, Monitoring plant and soil water status: established and novel methods revisited and their relevance to studies of drought tolerance, J. Exp. Bot. 58 (2) (2007) 119–130, https://doi.org/10.1093/jxb/erl118.

[77] M. Centritto, M. Lauteri, M.C. Monteverdi, R. Serraj, Leaf gas exchange, carbon isotope discrimination, and grain yield in contrasting rice genotypes subjected to water deficits during the reproductive stage, J. Exp. Bot. 60 (8) (2009) 2325–2339, https://doi.org/10.1093/jxb/erp123.

[78] V. Sibounheuang, J. Basnayake, S. Fukai, M. Cooper, Leaf-water potential as a drought resistance character in rice. Increased lowland rice production in the Mekong Region: Proceedings of an International Workshop held in Vientiane, Laos, 30 October-2 November 2000, Australian Centre for International Agricultural Research (ACIAR)., 2001, pp. 86–95.

[79] V. Sibounheuang, J. Basnayake, S. Fukai, Genotypic consistency in the expression of leaf water potential in rice (*Oryza sativa* L.), Field Crops Res. 97 (2–3) (2006) 142–154.

[80] C. Scoffoni, C. Vuong, S. Diep, H. Cochard, L. Sack, Leaf shrinkage with dehydration: coordination with hydraulic vulnerability and drought tolerance, Plant Physiol. 164 (4) (2014) 1772–1788, https://doi.org/10.1104/pp.113.221424. Epub 2013 Dec 4. PMID: 24306532; PMCID: PMC3982740.

[81] S. Peng, A.M. Ismail, Physiology basis of yield and environmental adaptation in rice, in: H.T. Nguyen, A. Blum (Eds.), Physiology and biotechnology integration for plant breeding, Marcel Dekker, New York, 2004, pp. 72–118.

[82] T. Takai, S. Adachi, F. Taguchi-Shiobara, et al., A natural variant of NAL1, selected in high-yield rice breeding programs, pleiotropically increases photosynthesis rate, Sci. Rep. 3 (2013) 2149.

[83] A. Afzal, S.W. Duiker, J.E. Watson, Leaf thickness to predict plant water status, Biosyst. Eng. 156 (2017) 148–156, https://doi.org/10.1016/j.biosystemseng.2017.01.011.

[84] N. Yadav, A.C.M.V. Sevanthi, R. Pandey, V. Chinnusamy, A.K. Singh, N.K. Singh, Physiological response and agronomic performance of drought tolerance mutants of Aus rice cultivar Nagina 22 (*Oryza sativa* L), Field Crops Res. 290 (2023) 108760. ISSN 0378-4290.

[85] L. Jian, K. Kang, Y. Choi, M.C. Suh, N.C. Paek, Mutation of OsMYB60 reduces rice resilience to drought stress by attenuating cuticular wax biosynthesis, Plant. J. 112 (2) (2022) 339–351, https://doi.org/10.1111/tpj.15947. Epub 2022 Sep 6. PMID: 35984735. [missed].

[86] G.P. John, C. Scoffoni, L. Sack, Allometry of cells and tissues within leaves, Am. J. Bot. 100 (10) (2013) 1936–1948.

[87] W. Ouyang, X. Yin, J. Yang, P.C. Struik, Do shoot anatomical characteristics allow rice to grow well under water deficit? J. Agron. Crop. Sci. 208 (2022) 763–776, https://doi.org/10.1111/jac.12509.

[88] G.P. John, C. Scoffoni, T.N. Buckley, R. Villar, H. Pooter, L. Sack, The anatomical and compositional basis of leaf mass per area, Ecol. Lett. 20 (4) (2017) 412–425.

[89] G. Pantuwan, S. Fukai, M. Cooper, S. Rajatasereekul, J.C. O'Toole, Yield response of rice (*Oryza sativa* L.) genotypes to drought under rainfed lowland: 3. Plant factors contributing to drought resistance, Field Crops Res. 73 (2-3) (2002) 181–200, https://doi.org/10.1016/S0378-4290(01)00194-0.

[90] T. Monkham, B. Jongdee, G. Pantuwan, J. Sanitchon, J.H. Mitchell, S. Fukai, Genotypic variation in grain yield and flowering pattern in terminal and intermittent drought screening methods in rainfed lowland rice, Field Crops Res. 175 (2015) 26–36.

[91] Y. Yi, H.A. Muhammad, C. Xinxin, Y. Li, H. Liu, W. Fang, Q. Zhu, S. Wang, QTL mapping and analysis for drought tolerance in rice by genome-wide association study (DOI=), Front. Plant. Sci. 14 (2023), https://doi.org/10.3389/fpls.2023.1223782.

[92] G. Pantuwan, S. Fukai, M. Cooper, S. Rajatasereekul, J.C.O.' Toole, J. Basnayake, Yield response of rice (*Oryza sativa* L.) genotypes to drought under rainfed lowlands 4, Veg. Stage Screen. Dry. Seas. Field Crops Res. 89 (2004) 281–297.

[93] A. Shekoofa, T.R. Sinclair, Aquaporin Activity to Improve Crop Drought Tolerance, Cells 7 (9) (2018) 123, https://doi.org/10.3390/cells7090123. PMID: 30158445; PMCID: PMC6162707.

[94] D. Labarga, A. Mairata, M. Puelles, I. Martín, A. Albacete, E. García-Escudero, A. Pou, The Rootstock Genotypes Determine Drought Tolerance by Regulating Aquaporin Expression at the Transcript Level and Phytohormone Balance, Plants (Basel) 12 (4) (2023) 718, https://doi.org/10.3390/plants12040718. PMID: 36840066; PMCID: PMC9961603.

[95] L. Wang, Q.T. Li, Q. Lei, et al., Ectopically expressing MdPIP1;3, an aquaporin gene, increased fruit size and enhanced drought tolerance of transgenic tomatoes, BMC Plant Biol. 17 (2017) 246, https://doi.org/10.1186/s12870-017-1212-2.

[96] J. He, W. Hu, H. Zhu, Y. Li, J. Zou, W.A. Khattak, Z. Zhou, Changes in cotton water use efficiency and its mechanism during drought and subsequent rehydration, Environ. Exp. Bot. 209 (2023) 105285, https://doi.org/10.1016/j.envexpbot.2023.105285.

[97] M.M. Kurowska, Aquaporins in cereals—important players in maintaining cell homeostasis under abiotic stress, Genes 12 (2021) 477, https://doi.org/10.3390/genes12040477.

[98] J. Bai, X. Wang, X. Yao, X. Chen, K. Lu, Y. Hu, Z. Wang, Y. Mu, L. Zhang, H. Dong, Rice aquaporin OsPIP2;2 is a water-transporting facilitator in relevance to drought-tolerant responses, Plant. Direct 16 5 (8) (2021) e338, https://doi.org/10.1002/pld3.338. PMID: 34430793; PMCID: PMC8365552.

[99] A. Grondin, R. Mauleon, V. Vadez, A. Henry, Root aquaporins contribute to whole plant water fluxes under drought stress in rice (*Oryza sativa* L.), Plant Cell Environ. 39 (2) (2016) 347–365, https://doi.org/10.1111/pce.12616. Epub 2015 Nov 24. PMID: 26226878.

[100] N.M. Hassan, Z.M. El-Bastawisy, A.K. El-Sayed, H.T. Ebeed, M.M. Nemat Alla, Roles of dehydrin genes in wheat tolerance to drought stress, J. Adv. Res. 6 (2) (2015) 179–188, https://doi.org/10.1016/j.jare.2013.11.004. Epub 2013 Nov 21. PMID: 25750752; PMCID: PMC4348445.

[101] Z. Sun, S. Li, W. Chen, J. Zhang, L. Zhang, W. Sun, Z. Wang, Plant Dehydrins: Expression, Regulatory Networks, and Protective Roles in Plants Challenged by Abiotic Stress, Int. J. Mol. Sci. 22 (23) (2021) 12619, https://doi.org/10.3390/ijms222312619. PMID: 34884426; PMCID: PMC8657568.

[102] M. Kumar, S.C. Lee, J.Y. Kim, et al., Over-expression of dehydrin gene, *OsDhn1*, improves drought and salt stress tolerance through scavenging of reactive oxygen species in rice (*Oryza sativa L.*), J. Plant Biol. 57 (2014) 383–393, https://doi.org/10.1007/s12374-014-0487-1.

[103] Thalmann, Santelia, Starch as a determinant of plant fitness under abiotic stress, New Phytol. 214 (2017) 943–995.

[104] M. Guo, H. Zhao, Z. He, W. Zhang, Z. She, M.A. Mohammadi, C. Shi, M. Yan, D. Tian, Y. Qin, Comparative Expression Profiling of Snf2 Family Genes During Reproductive Development and Stress Responses in Rice, Front. Plant Sci. 13 (2022) 910663, https://doi.org/10.3389/fpls.2022.910663.

[105] Y.S. Yang, C. Li, T. Hu, S. Hou, Q. Bai, X. Ji, F. Xu, C. Guo, M. Huang, Y. Cai, J. Liu, The plasma membrane-localized OsNIP1;2 mediates internal aluminum detoxification in rice, Front. Plant Sci. 12 (13) (2022) 970270, https://doi.org/10.3389/fpls.2022.970270. PMID: 36172551; PMCID: PMC9512054.

[106] H. Eryong, S. Bo, OsABT, a Rice WD40 Domain-Containing Protein, Is Involved in Abiotic Stress Tolerance, ISSN 1672-6308, Rice Sci. 29 (3) (2022) 247–256, https://doi.org/10.1016/j.rsci.2021.07.012.

[107] R. Hu, J. Xiao, T. Gu, X. Yu, Y. Zhang, J. Chang, G. Yang, G. He, Correction to: Genome-wide identification and analysis of WD40 proteins in wheat (Triticum aestivum L.), BMC Genom. 19 (2018) 852.

[108] W. Lin, Y. Wang, X. Liu, J.X. Shang, L. Zhao, OsWAK112, A Wall-Associated Kinase, Negatively Regulates Salt Stress Responses by Inhibiting Ethylene Production, Front. Plant Sci. 5 (12) (2021) 751965, https://doi.org/10.3389/fpls.2021.751965. PMID: 34675955; PMCID: PMC8523997.

[109] S. Campo, P. Baldrich, J. Messeguer, E. Lalanne, M. Coca San, B. Segundo, Overexpression of a Calcium-Dependent Protein Kinase confers Salt and Drought Tolerance in Rice by Preventing Membrane Lipid Peroxidation, Plant Physiol. 165 (2) (2014) 688–704, https://doi.org/10.1104/pp.113.230268. Epub 2014 May 1. PMID: 24784760; PMCID: PMC4044838.

[110] S. Wei, W. Hu, X. Deng, et al., A rice calcium-dependent protein kinase OsCPK9 positively regulates drought stress tolerance and spikelet fertility, BMC Plant Biol. 14 (2014) 133, https://doi.org/10.1186/1471-2229-14-133.

[111] M. Liu, X. Li, Y. Liu, B. Cao, Regulation of flavanone 3-hydroxylase gene involved in the flavonoid biosynthesis pathway in response to UV-B radiation and drought stress in the desert plant, *Reaumuria soongorica*, Plant Physiology Biochemistry PPB / Societe francaise de physiologie vegetale 73C (2013) 161–167, https://doi.org/10.1016/j.plaphy.2013.09.016.

[112] S.K. Dwivedi, S. Kumar, M.A. Natividad, et al., Disentangling the Roles of Plant Water Status and Stem Carbohydrate Remobilization on Rice Harvest Index Under Drought, Rice 16 (2023) 14, https://doi.org/10.1186/s12284-023-00631-6.

[113] Q. Long, S. Qiu, J. Man, et al., OsAAI1 increases rice yield and drought tolerance dependent on ABA-mediated regulatory and ROS scavenging pathway, Rice 16 (35) (2023), https://doi.org/10.1186/s12284-023-00650-3.

[114] W.Y. Liu, M.M. Wang, J. Huang, H.J. Tang, H.X. Lan, H.S. Zhang, The OsDHODH1 gene is involved in salt and drought tolerance in rice, J. Integr. Plant. Biol. 51 (9) (2009) 825–833, https://doi.org/10.1111/j.1744-7909.2009.00853.x.
[115] S. Liu, L. Zhao, M. Cheng, J. Sun, X. Ji, A. Ullah, G. Xie, Calmodulins and calmodulin-like proteins-mediated plant organellar calcium signaling networks under abiotic stress, Crop J. 12 (5) (2024) 1321–1332.
[116] E. Baldoni, A. Genga, E. Cominelli, Plant *MYB* Transcription Factors: Their Role in Drought Response Mechanisms, Int. J. Mol. Sci. 16 (7) (2015) 15811–15851, https://doi.org/10.3390/ijms160715811. PMID: 26184177; PMCID: PMC4519927.
[117] N.Q. Dong, Y. Sun, T. Guo, et al., UDP-glucosyltransferase regulates grain size and abiotic stress tolerance associated with metabolic flux redirection in rice, Nat. Commun. 11 (2020) 2629, https://doi.org/10.1038/s41467-020-16403-5.
[118] Z. Wang, Y. Yang, V. Yadav, W. Zhao, Y. He, X. Zhang, C. Wei, Drought-induced proline is mainly synthesized in leaves and transported to roots in watermelon under water deficit, Hortic. Plant J. 8 (5) (2022) 615–626.
[119] T.R. Sinclair, Effective water use required for improving crop growth rather than transpiration efficiency, URL=https://www.frontiersin.org/journals/plant-science/articles/10.3389/fpls.2018.01442, Front. Plant. Sci. 9 (2018), https://doi.org/10.3389/fpls.2018.01442.
[120] R.E. Kramp, P. Liancourt, M. Herberich, L. Saul, S. Weides, K. Tielbörger, M. Májeková, Functional traits and their plasticity shift from tolerant to avoidant under extreme drought, Ecology 103 (12) (2022), https://doi.org/10.1002/ecy.3826.
[121] G.D. Farquhar, T.N. Buckley, J.M. Miller, Optimal stomatal control in relation to leaf area and nitrogen content, Silva Fenn. 36 (3) (2002) 625–637.